Outflowing gas around black holes modelled with CLOUDY/Xstar

Susmita Chakravorty

ANR-Chaos Fellow
Institut de Planétologie et d'Astrophysique de Grenoble

Collaborating with
Pierre-Olivier Petrucci, Jonathan Ferreira
Julia Lee, Gerard Kriss,
Martin Elvis, Gary Ferland, Ajit Kembhavi, Ranjeev Misra
Sibasish Laha, Matteo Guainazzi, Gulab Dewangan

Based on
Chakravorty et. al. 2009, MNRAS, 393, 83
Chakravorty et. al. 2012, MNRAS, 422, 637
Lee et.al. 2013, MNRAS, 430, 2650
Laha et.al. 2013, ApJ, 777, 2
Laha et.al. 2014, MNRAS, 441, 2613
Chakravorty et.al 2015 (submited to A&A)

CLOUDY workshopIUCAA
24th September, 2015

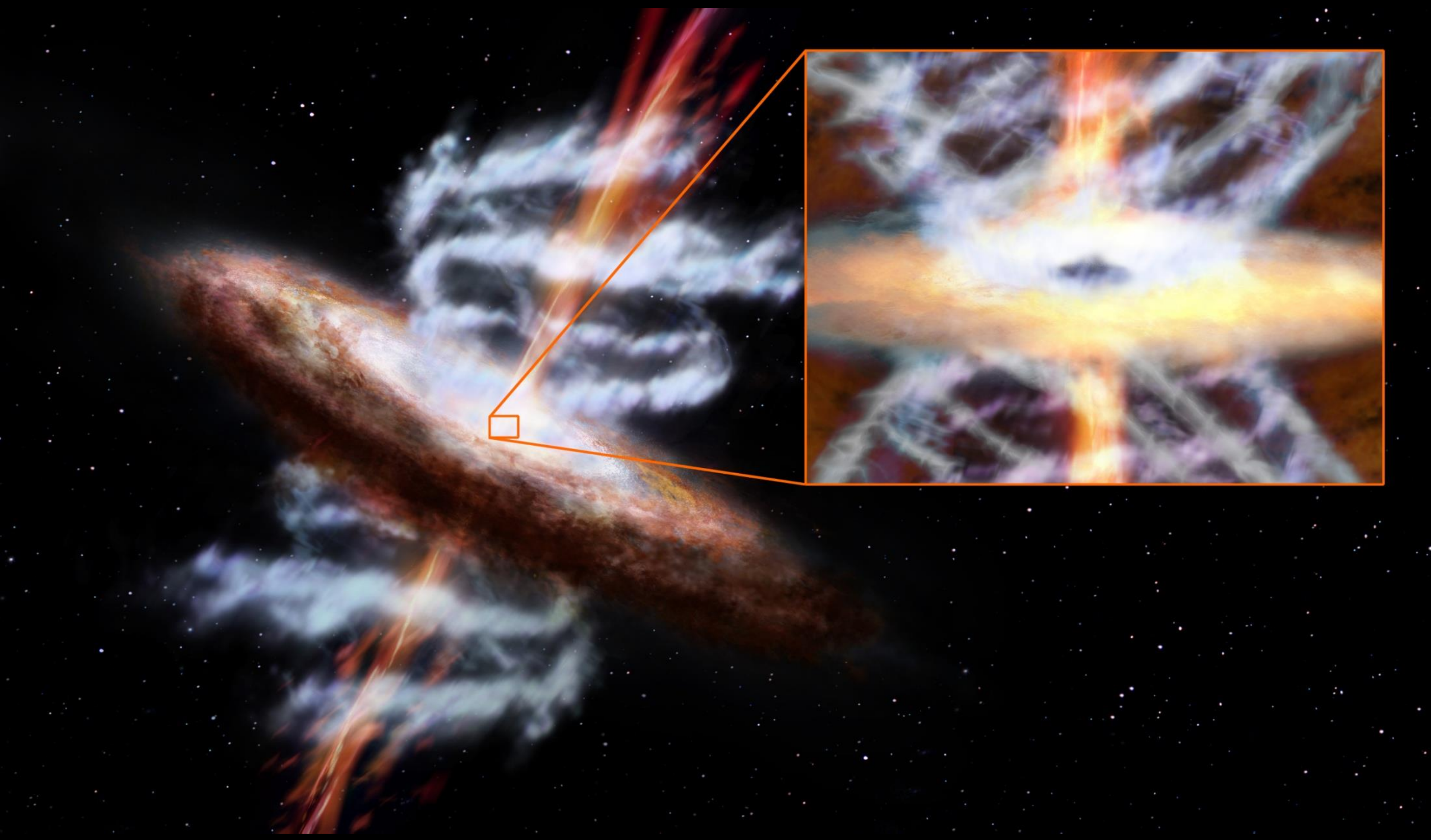

Artist concept credit: ESA/AOES Medialab

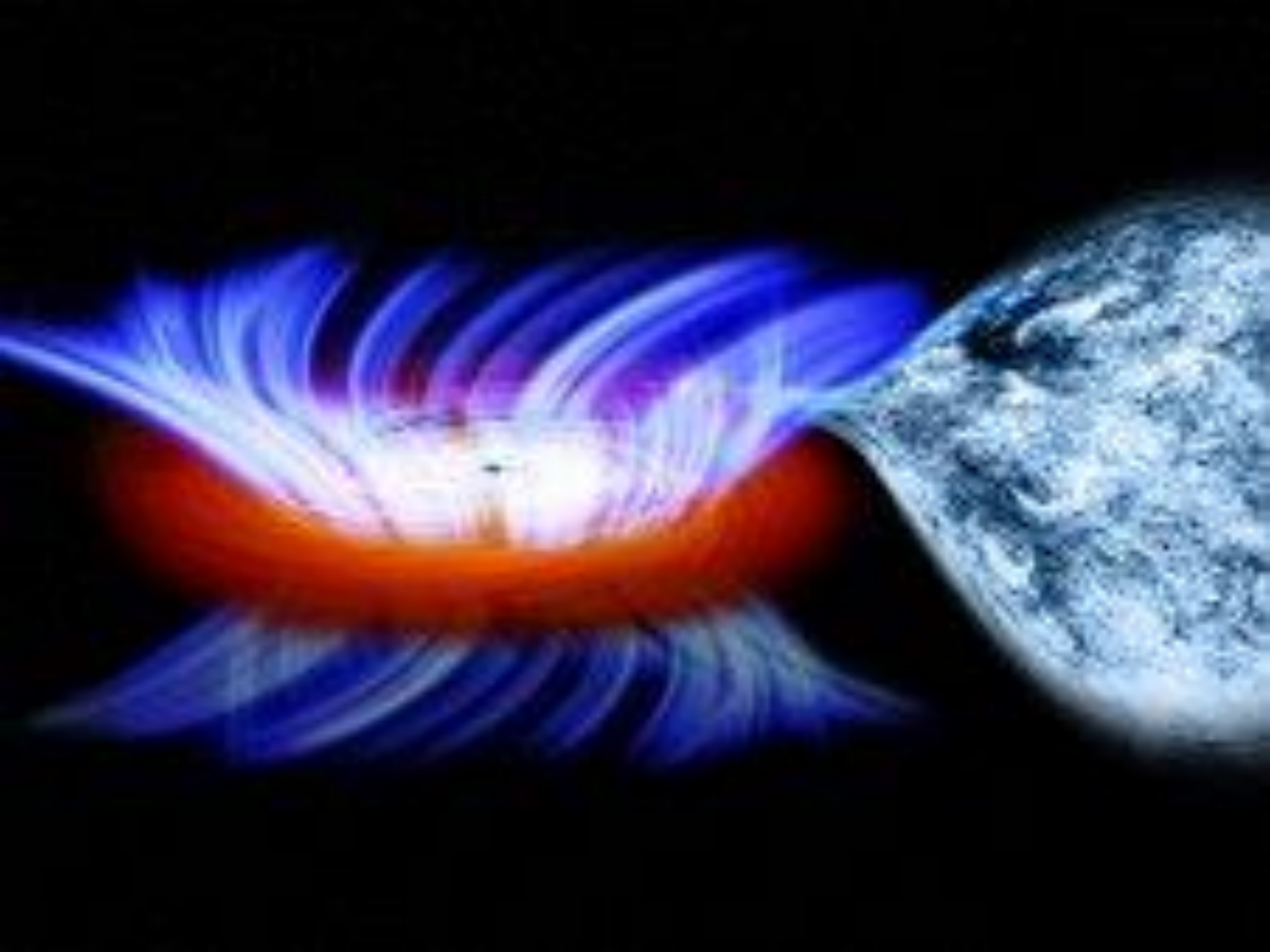

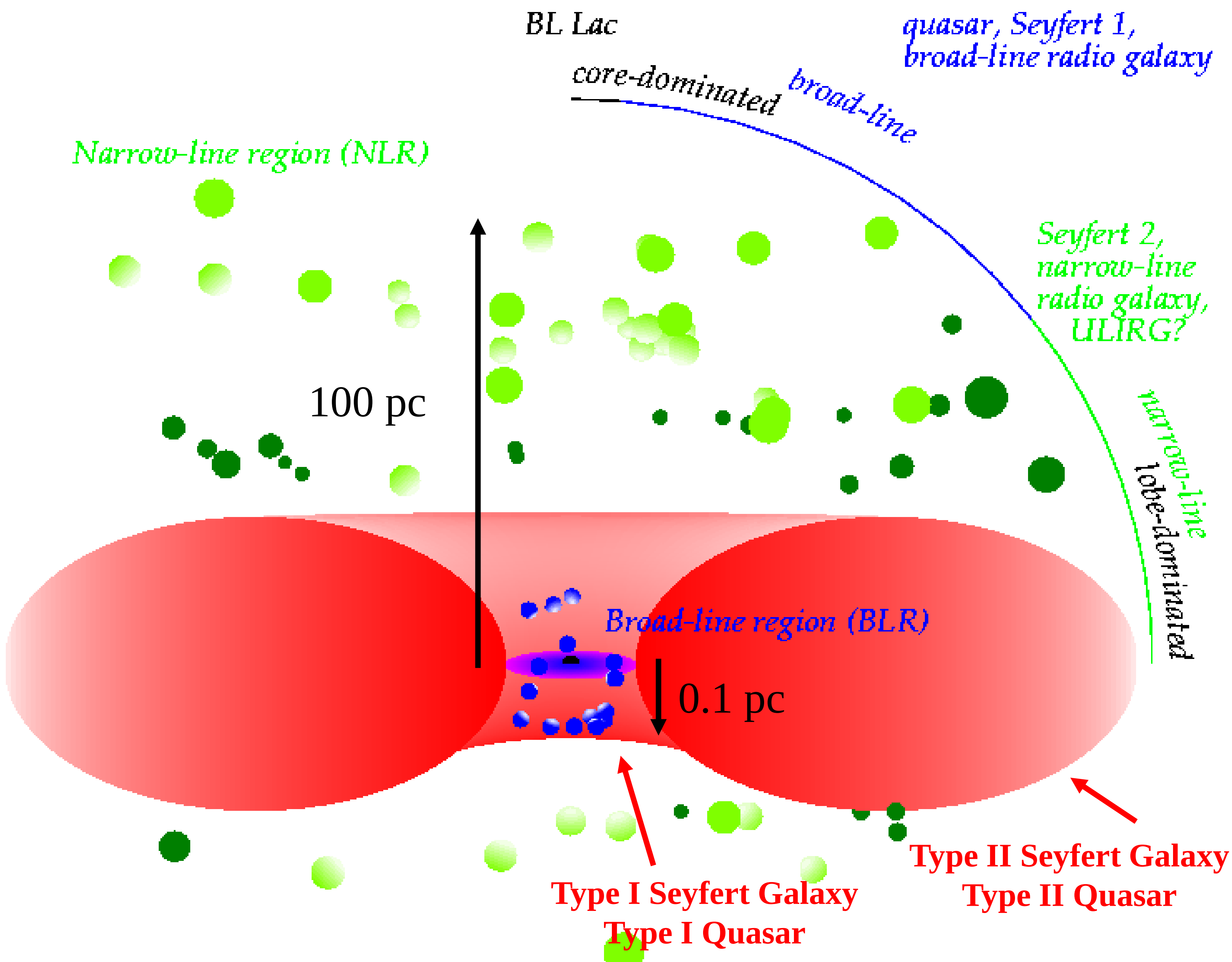

BL Lac
quasar, Seyfert 1,
broad-line radio galaxy
core-dominated
broad-line
Narrow-line region (NLR)
Seyfert 2,
narrow-line
radio galaxy,
ULIRG?
narrow-line
lobe-dominated
100 pc
Broad-line region (BLR)
0.1 pc
Type I Seyfert Galaxy
Type I Quasar
Type II Seyfert Galaxy
Type II Quasar

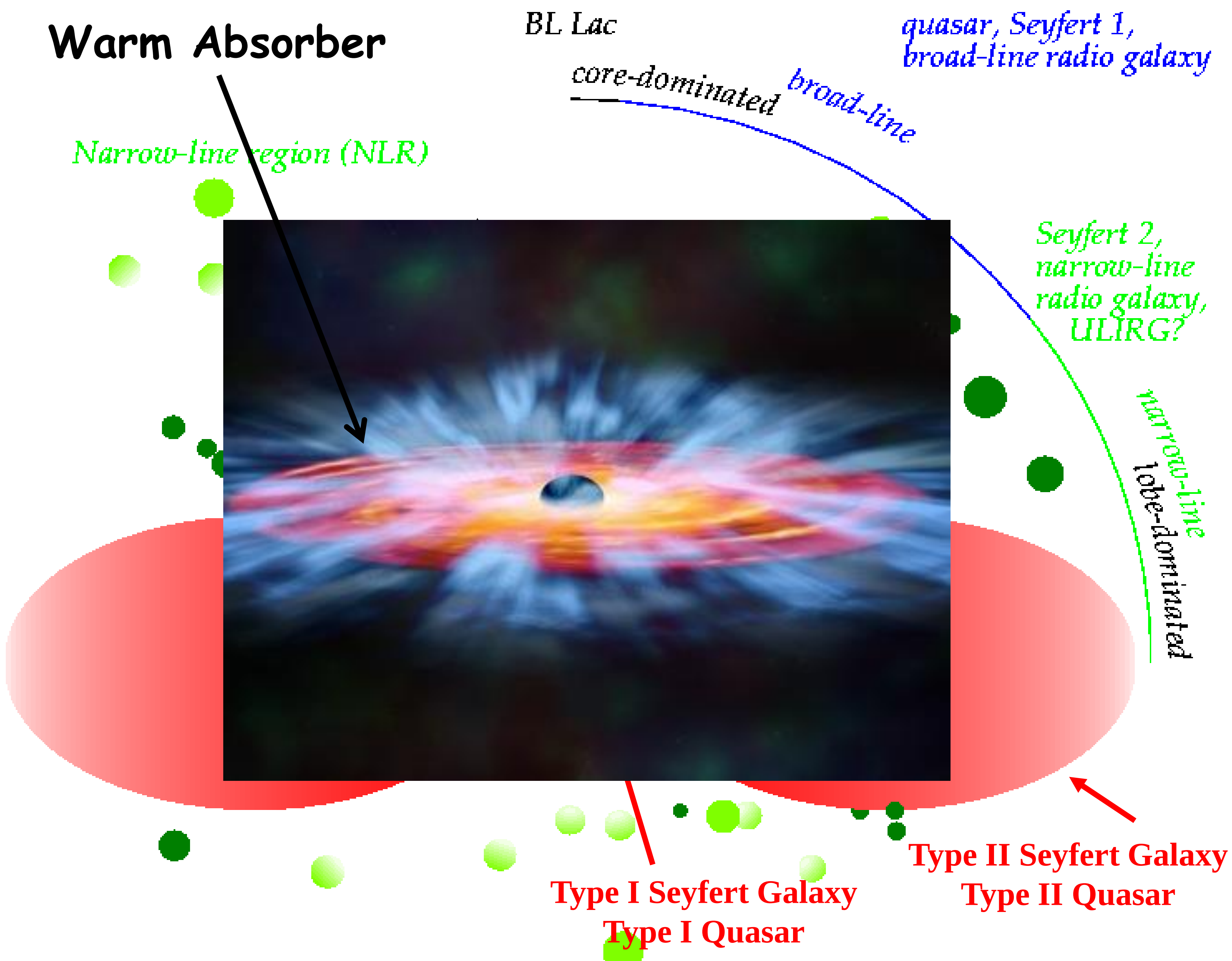

Warm Absorber
BL Lac
quasar, Seyfert 1,
broad-line radio galaxy
core-dominated
broad-line
Narrow-line region (NLR)
Seyfert 2,
narrow-line
radio galaxy,
ULIRG?
narrow-line
lobe-dominated
Type II Seyfert Galaxy
Type II Quasar
Type I Seyfert Galaxy
Type I Quasar

The different AGN outflows

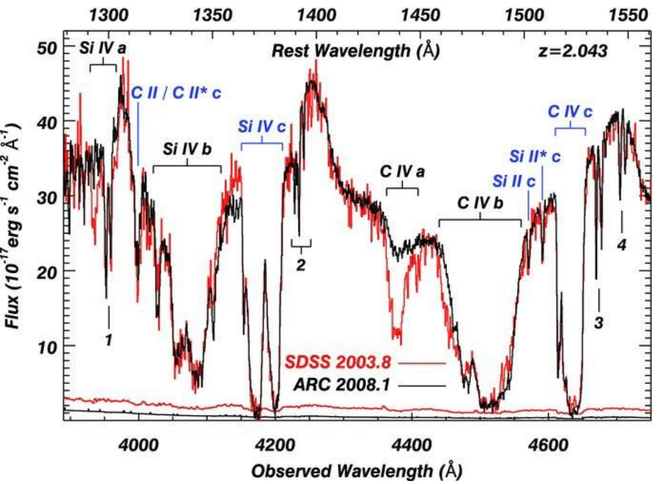

BAL QSOs in Optical
SDSS 0838+2955

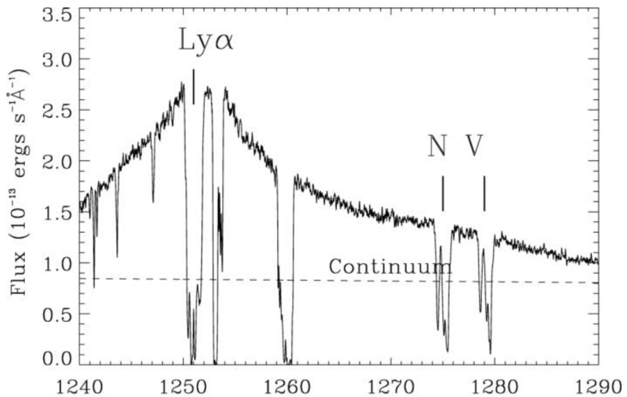

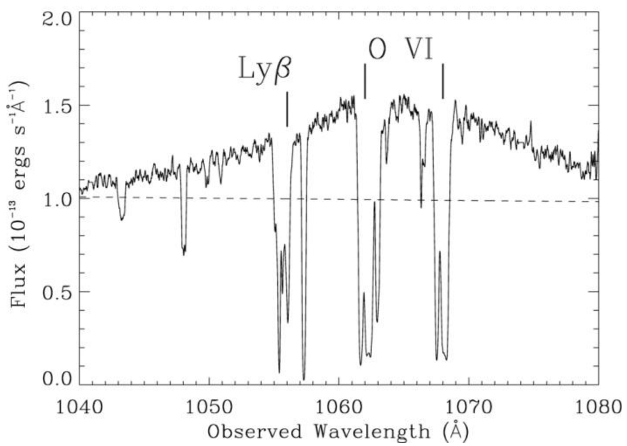

NAL QSOs in Ultraviolet (UV)
Mrk 279

The different AGN outflows

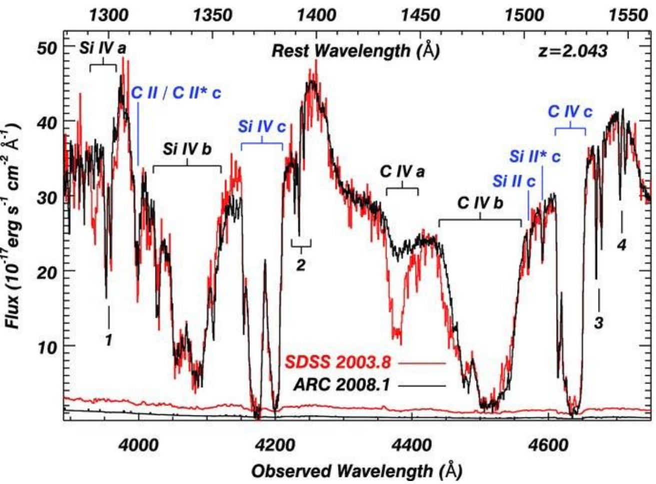

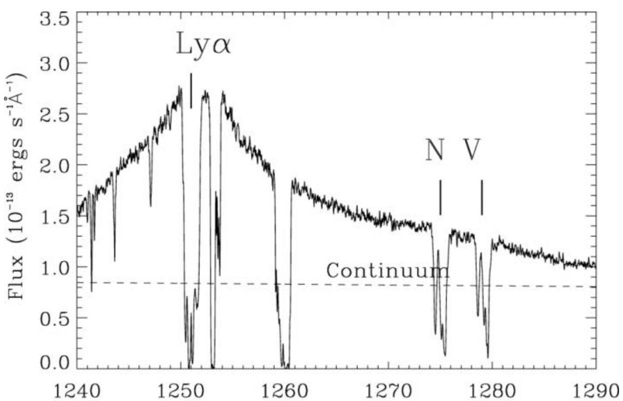

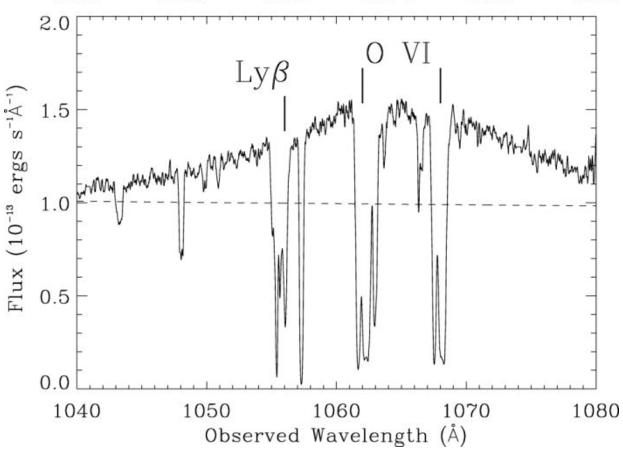

WAs in soft X-rays
IRAS 13349+2438

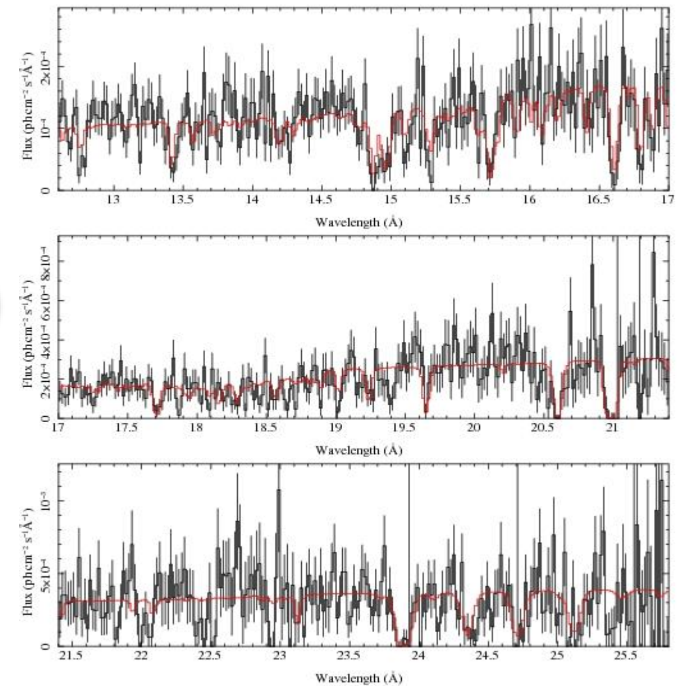

UFOs in 'high' soft-Xrays
PG1211+143

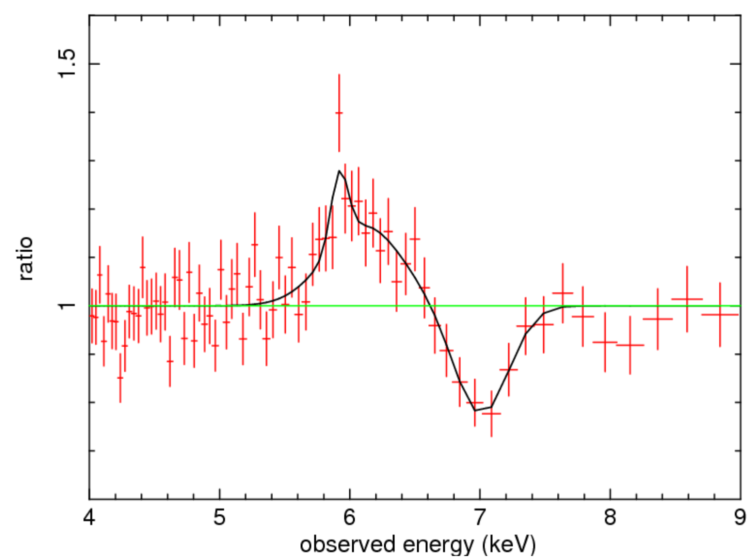

Broad Band Continuum

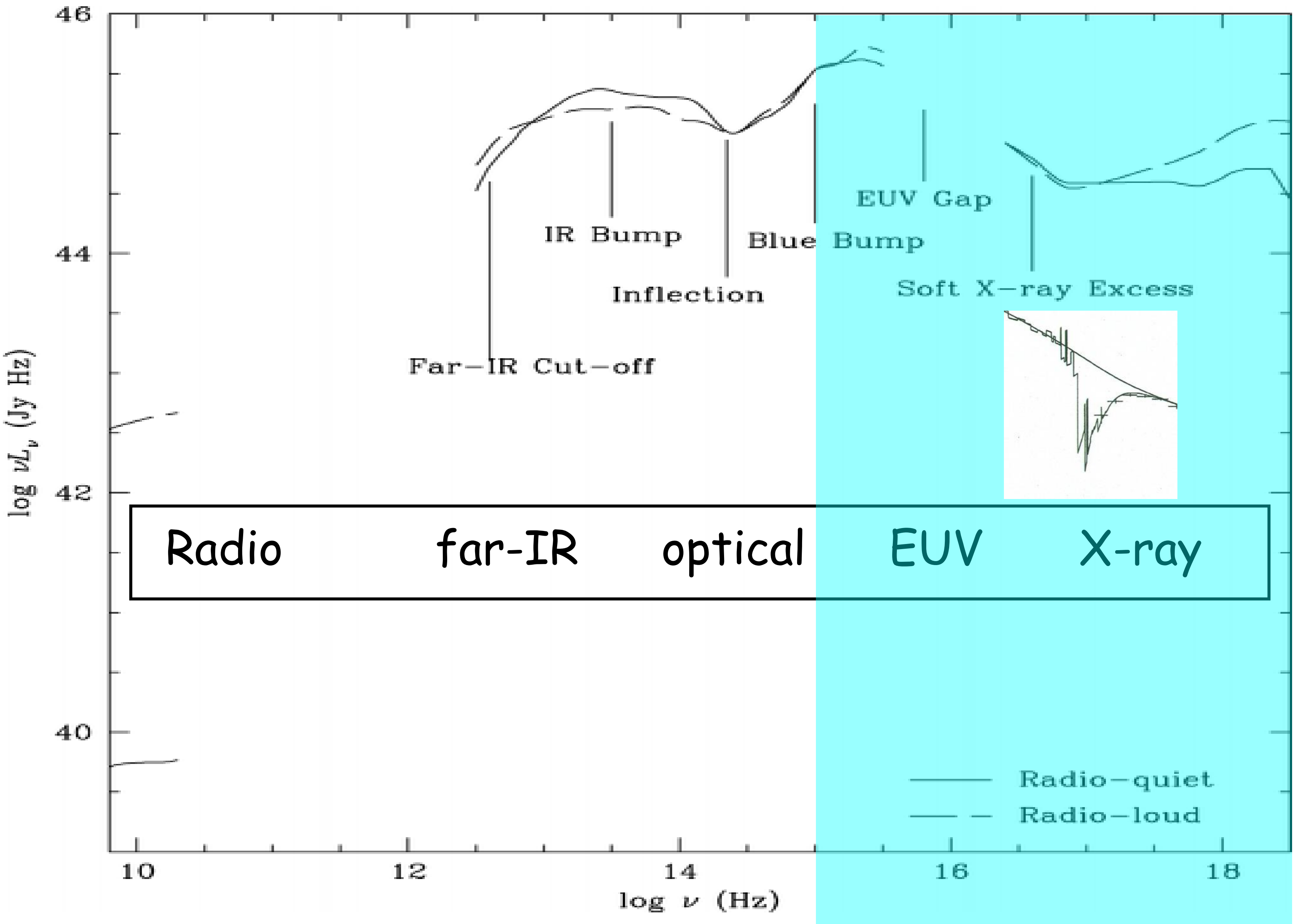

Warm Absorber

- Absorption features in Soft X-ray

C (V & VI) O (V - VIII) Fe (XVII - XXII)
Ne (IX & X) Mg (XI & XII) Al (XII & XIII)
Si (XIII - XVI) S (XV & XVI)

- Absorption features are blue shifted, indicating outflow.

- $N_H \sim 10^{22\pm1}$ cm^{-2}

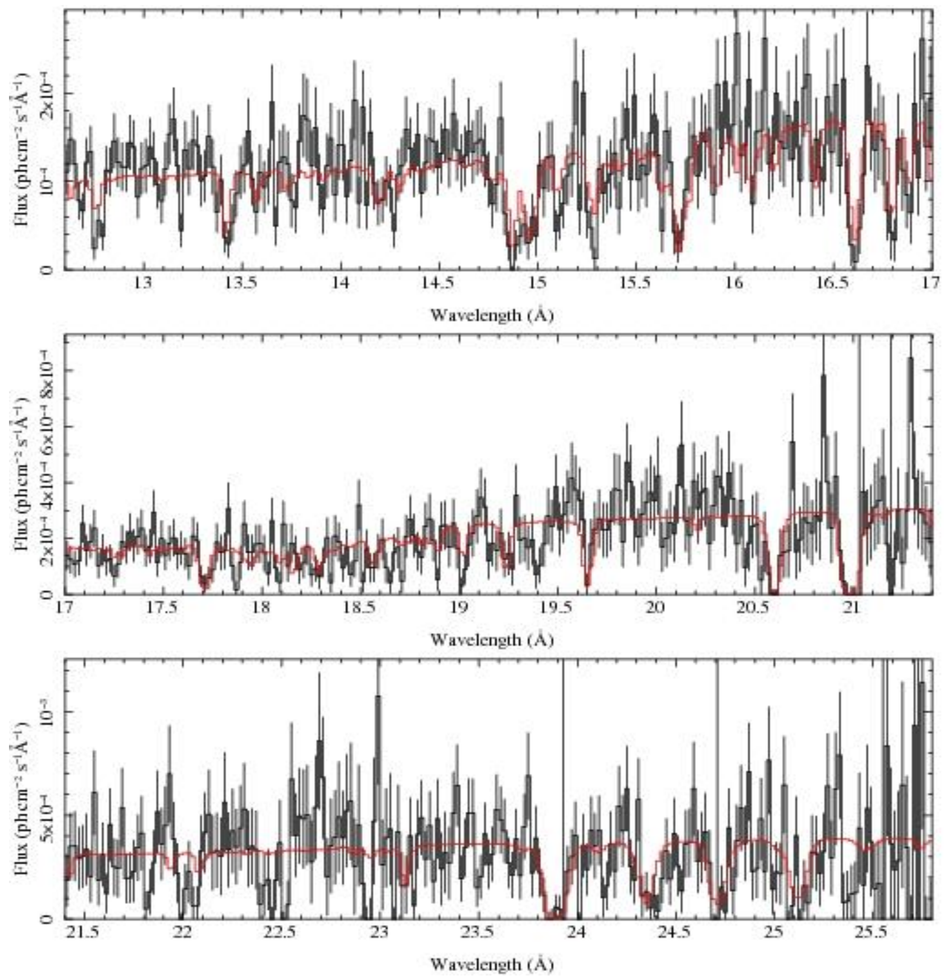

Warm Absorber

- Absorption features in Soft X-ray

C (V & VI)   O (V - VIII)   Fe (XVII - XXII)
Ne (IX & X)   Mg (XI & XII)   Al (XII & XIII)
Si (XIII - XVI)   S (XV & XVI)

- Absorption features are blue shifted, indicating outflow.

- $N_H \sim 10^{22\pm1}$ cm^{-2}

- $\xi = L/nR^2 \sim 10 - 1000$ erg cm s^{-1}

- $T_{gas} \sim 10^4$ K – $10^{6.5}$ K

- $n_H \sim 10^9$ cm^{-3} (10^5 - 10^{12})
  $R_{gas} \sim 0.01 - 100$ pc

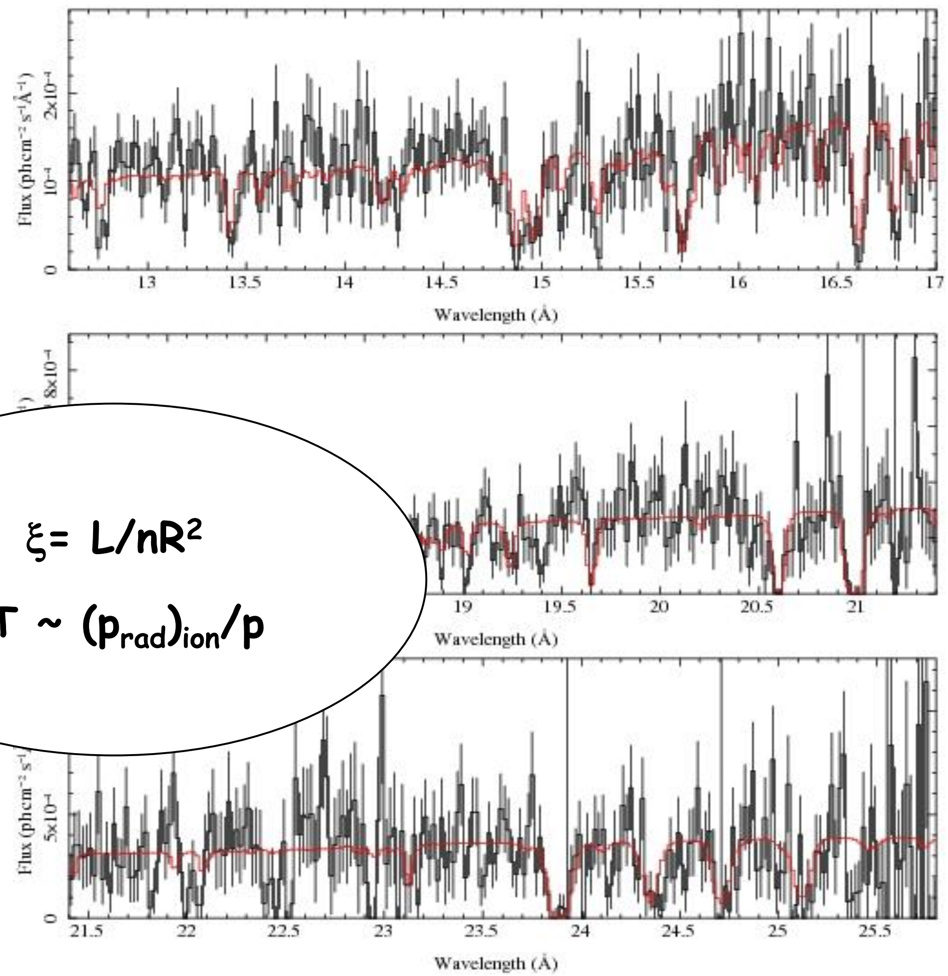

$\xi = L/nR^2$

$\xi/T \sim (p_{rad})_{ion}/p$

How photoionization modeling works

Cloudy table models or Warmabs * (Blackbody+Powerlaw)

Inputs

Radiation Field

Geometry

Abundance

Density

Thickness

Chandra HEG

Chandra MEG

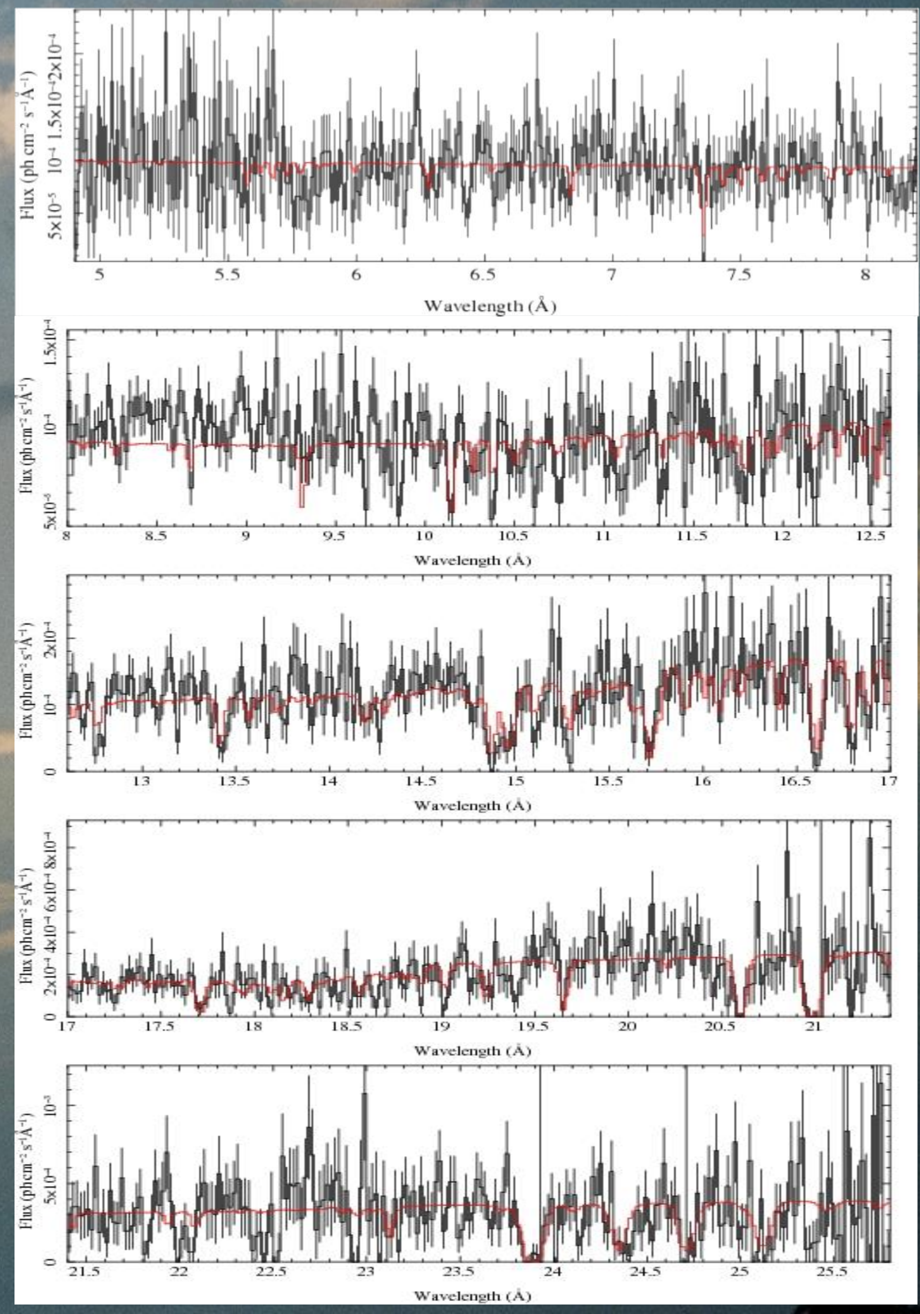

How photoionization modeling works

Cloudy table models or Warmabs * (Blackbody+Powerlaw)

Inputs

- Radiation Field
- Geometry
- Abundance
- Density
- Thickness

Process

Ionization balance

$$n(X^{+i})\Gamma(X^{+i}) = n(X^{+i+1})\, n_e\, \alpha_G(X^{+i+1}, T)$$

Photoionization cross-section

Recombination coefficient

Thermal balance

$$\Lambda_{Coll} + \Lambda_{IC} = (\Gamma_{Ph} + \Gamma_{C}) / n$$

Collisional cooling rates due to

Radiative recombination (free-bound)
Dielectronic recombination
Line excitation (bound-bound)

Inverse compton cooling rate

Photoionization heating rate

Compton heating rate

How photoionization codes Work

Cloudy table models
or
Warmabs

* (Blackbody+Powerlaw)

Output

Thermal state & Ionic composition of cloud

Inputs

Radiation Field

Geometry

Abundance

Density

Thickness

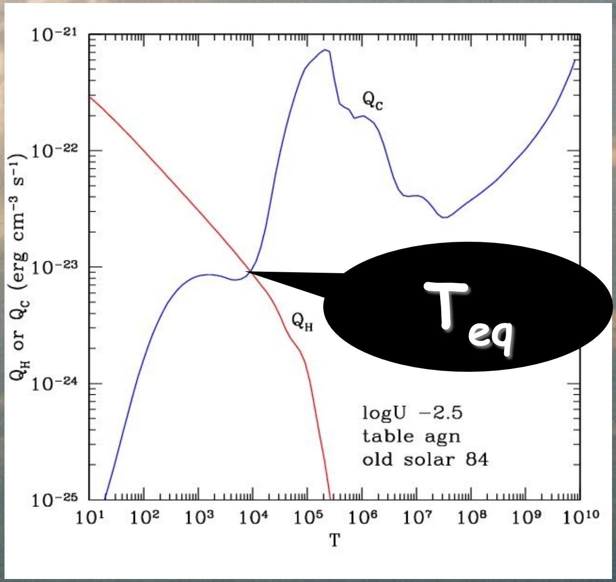

How photoionization codes Work

Cloudy table models
or
Warmabs

* (Blackbody+Powerlaw)

Inputs

Radiation Field

Geometry

Abundance

Density

Thickness

Output

<u>Thermal state</u> & <u>Ionic composition</u> of cloud

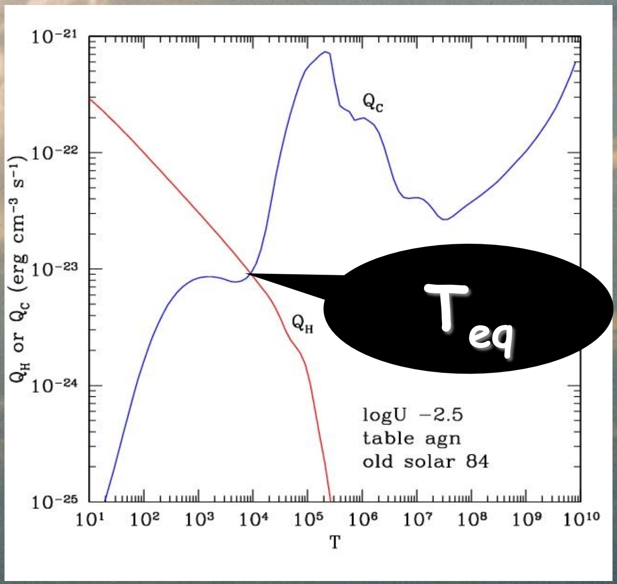

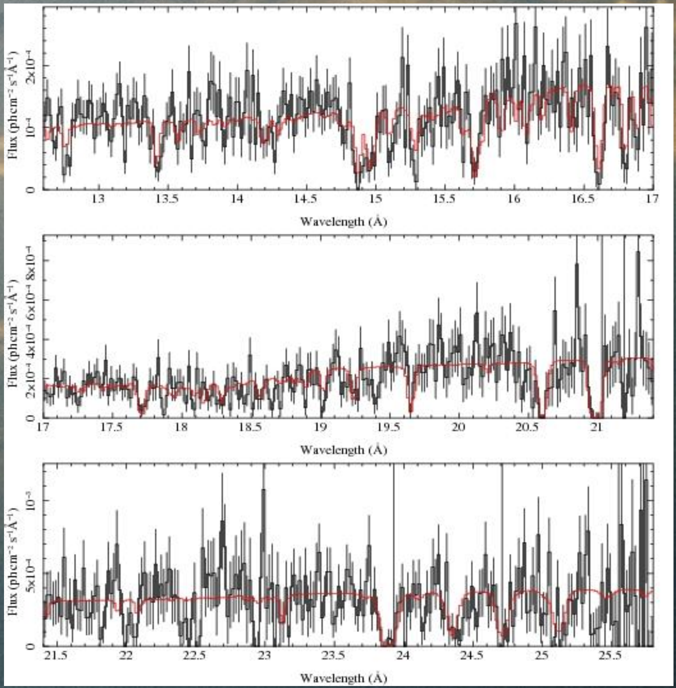

How photoionization codes Work

Cloudy table models or Warmabs * (Blackbody+Powerlaw)

Inputs

Radiation Field

Geometry

Abundance

Density

Thickness

Output

Thermal state & Ionic composition of cloud

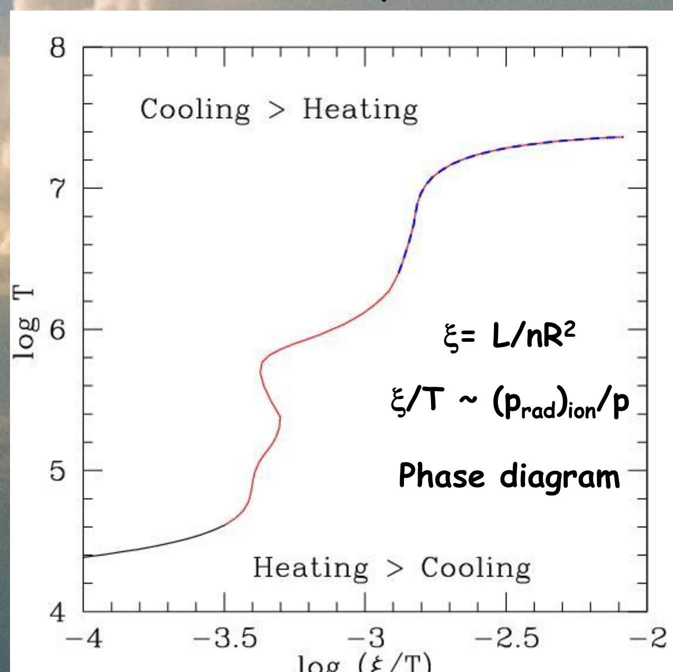

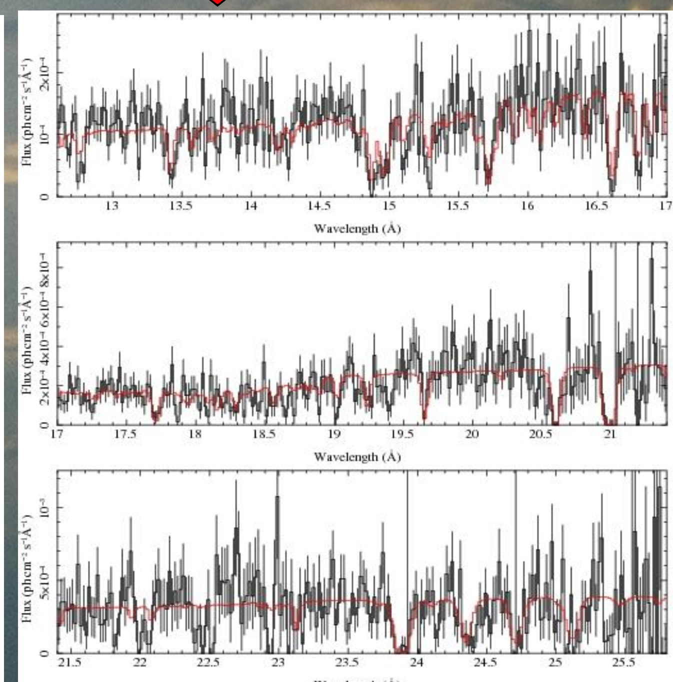

How photoionization codes Work

Cloudy table models or Warmabs

* (Blackbody+Powerlaw)

Inputs

Radiation Field

Geometry

Abundance

Density

Thickness

Output

Thermal state & Ionic composition of cloud

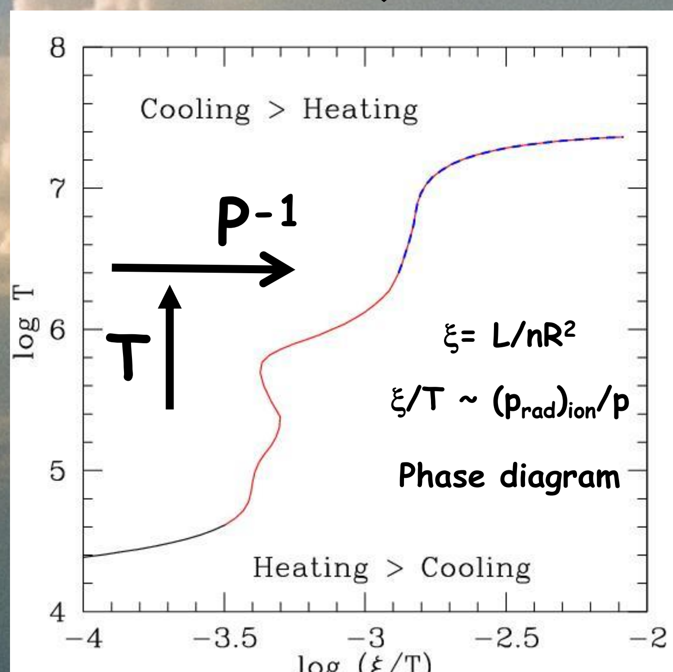

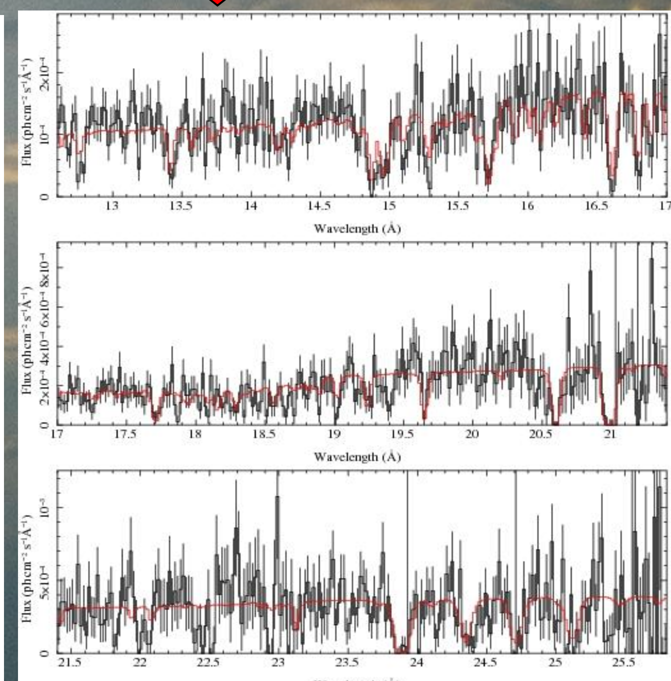

Relate Warm absorber and S-curve

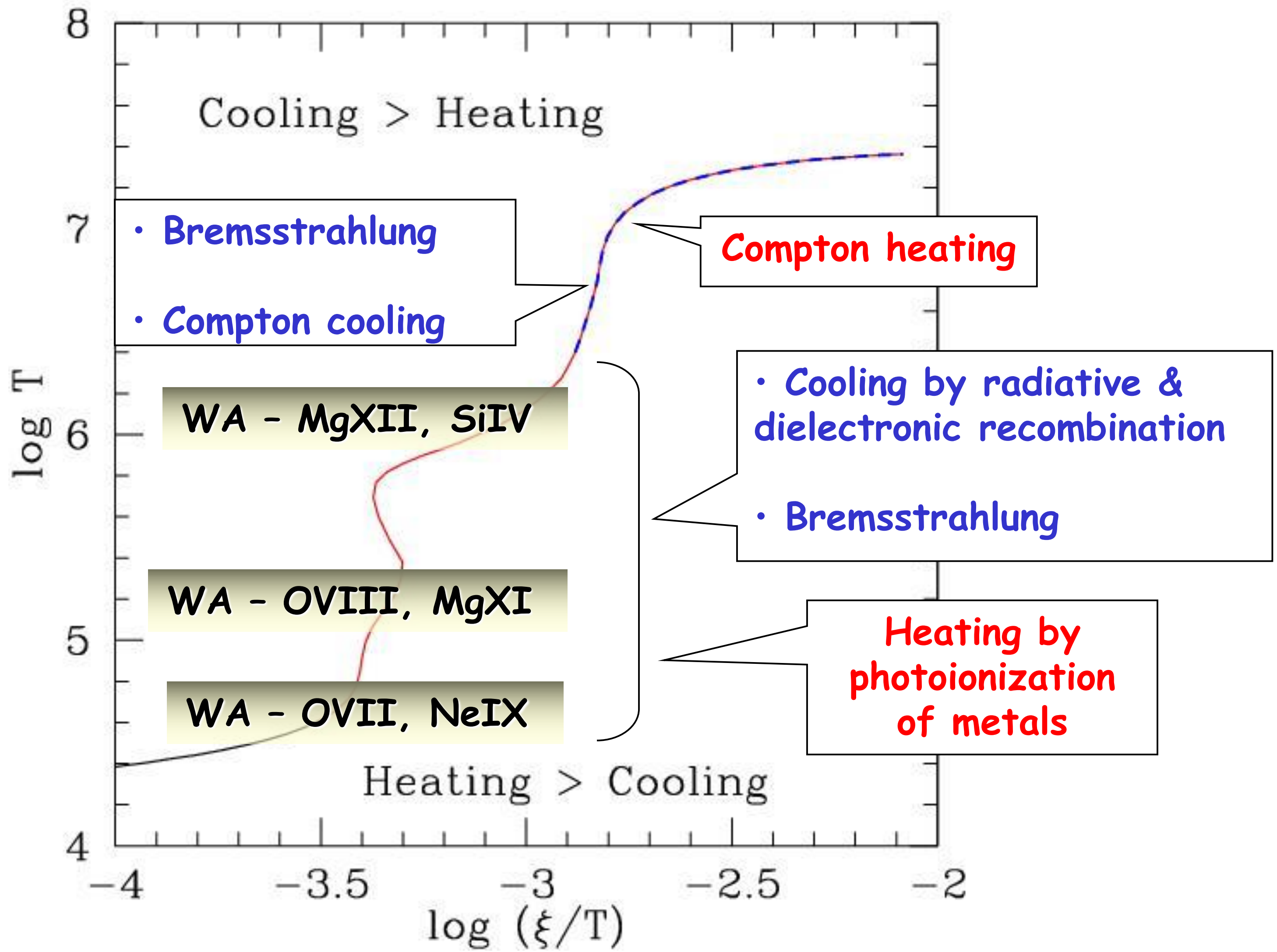

Multi-wavelength SED for IRAS 13349+2438

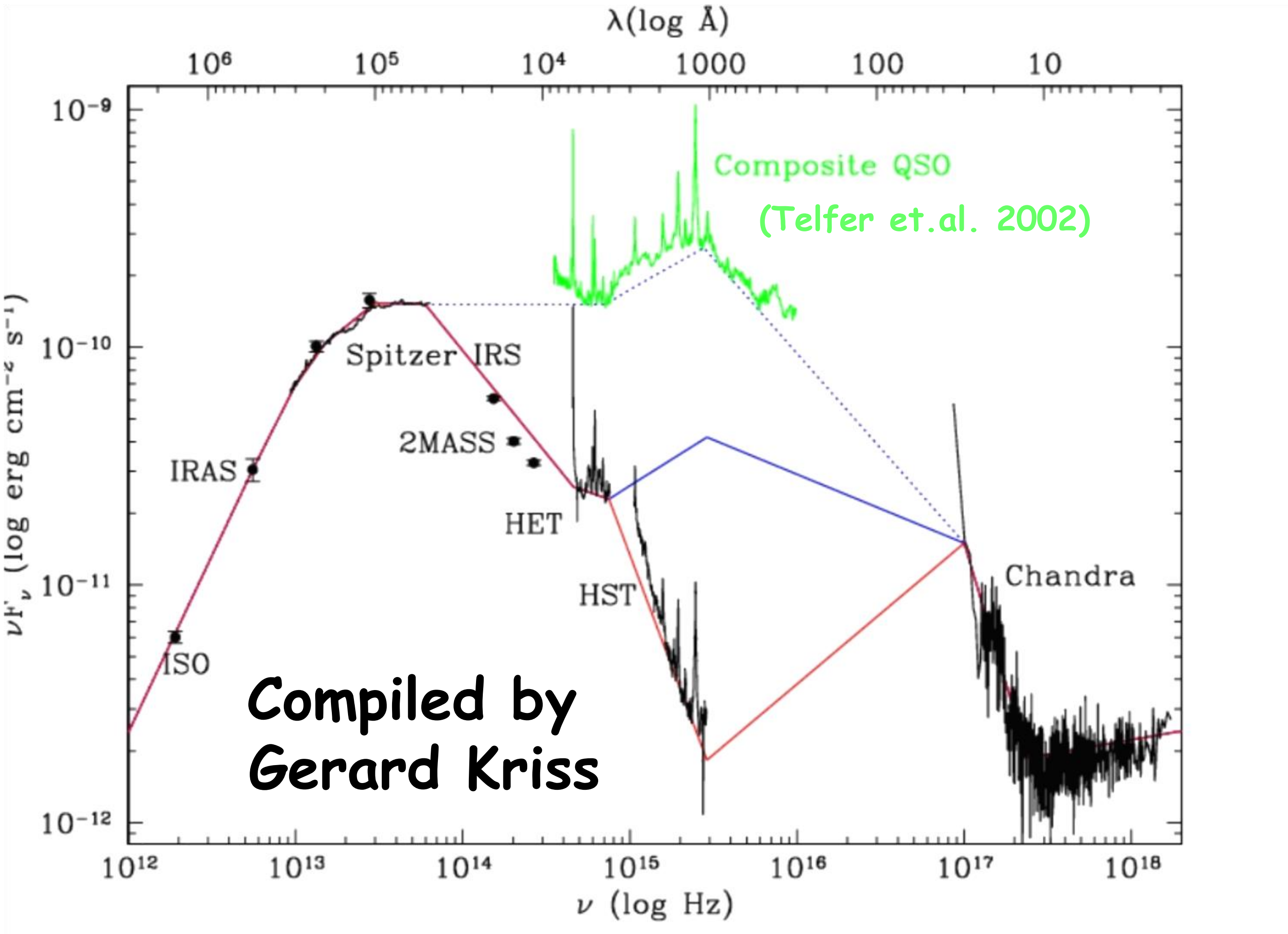

Multi-wavelength SED for IRAS 13349+2438

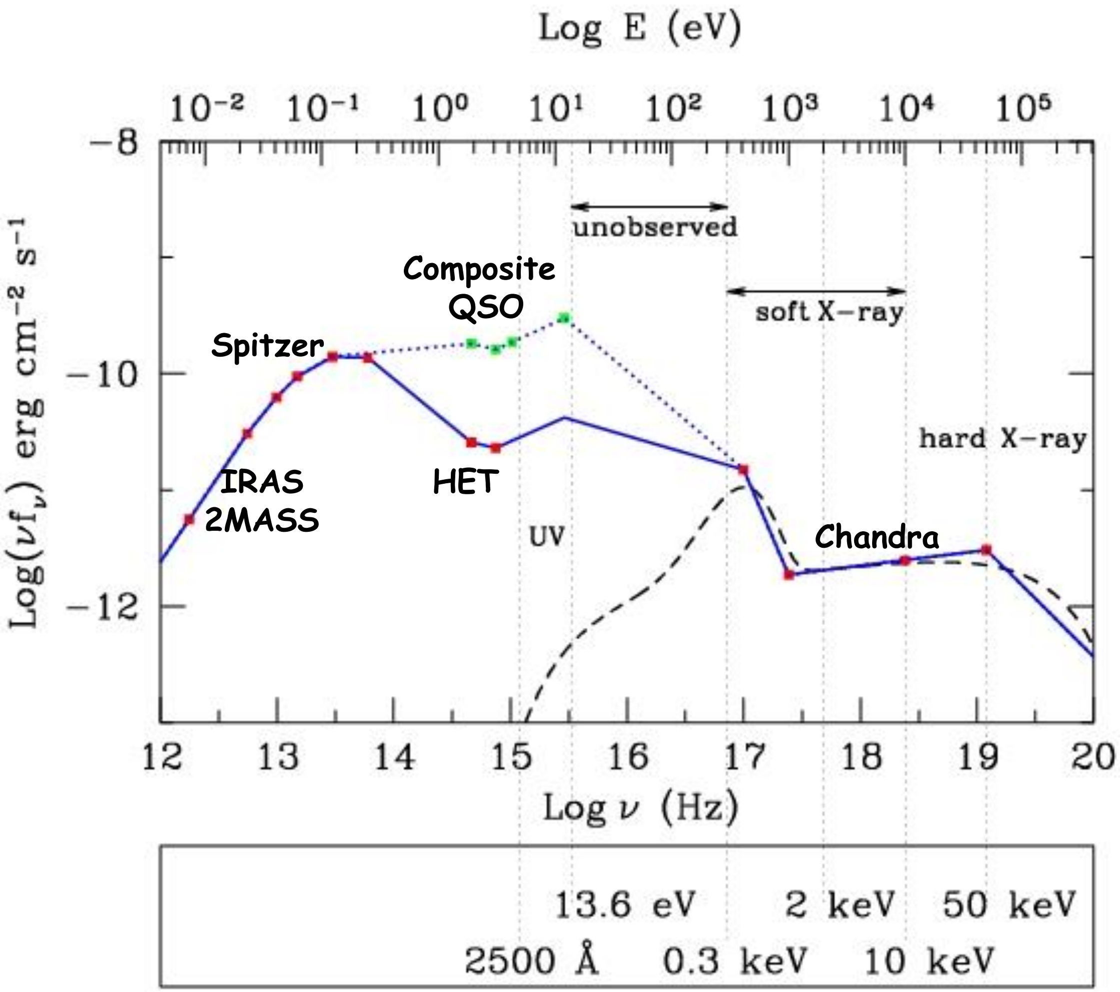

- Red filled squares are observed data points.
- Near simultaneous X-ray and Optical data.
- Infrared from Spitzer, 2MASS and IRAS.
- Green filled squares are `average SED for AGN' in UV (Telfer et.al. 2002).
- The blue lines are arbitrary, simplistic joins between EUV and X-ray.
- We wish to model the far UV part of the SED with "diskbb".

Multi-wavelength SED for IRAS 13349+2438

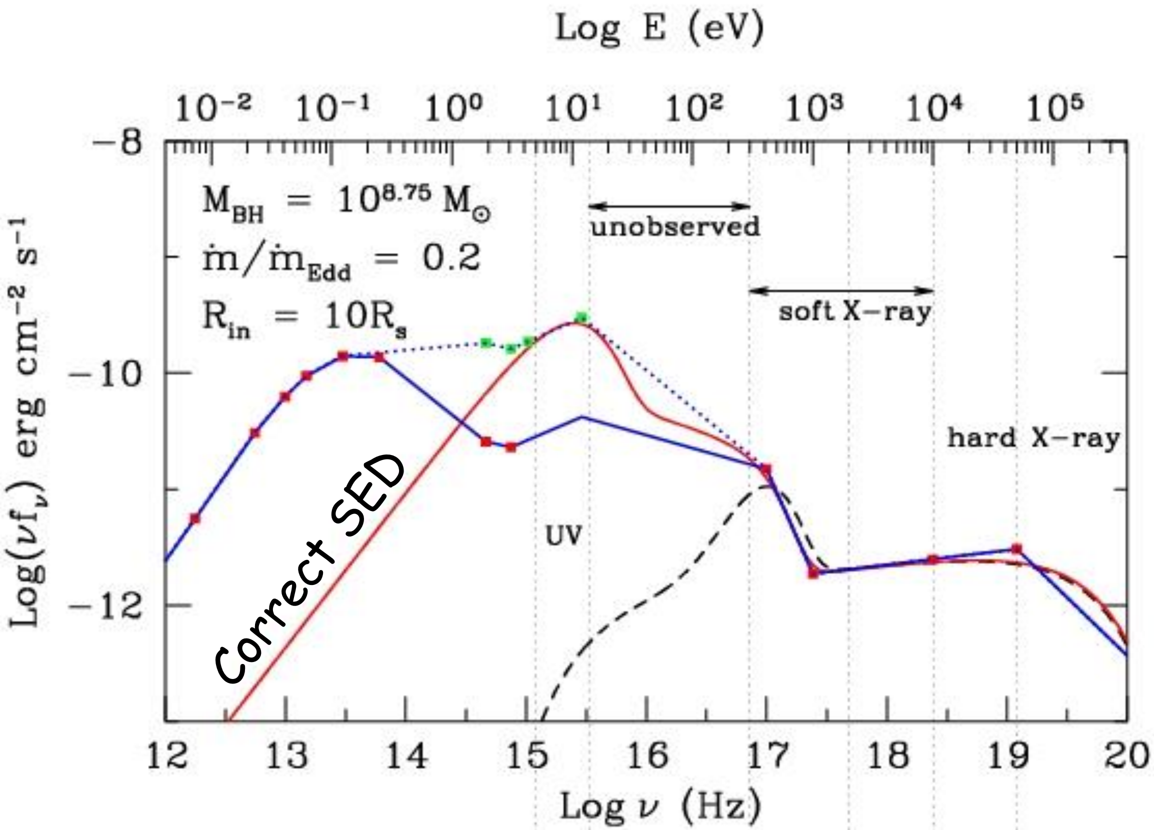

- Red filled squares are observed data points.
- Near simultaneous X-ray and Optical data.
- Infrared from Spitzer, 2MASS and IRAS.
- Green filled squares are `average SED for AGN' in UV (Telfer et.al. 2002).
- The blue lines are arbitrary, simplistic joins between EUV and X-ray.
- We wish to model the far UV part of the SED with "diskbb".

Hβ measurements – $M_{BH} \sim 10^{9.1}\ M_{sol}$

XSTAR warm absorber analysis using `correct' SED

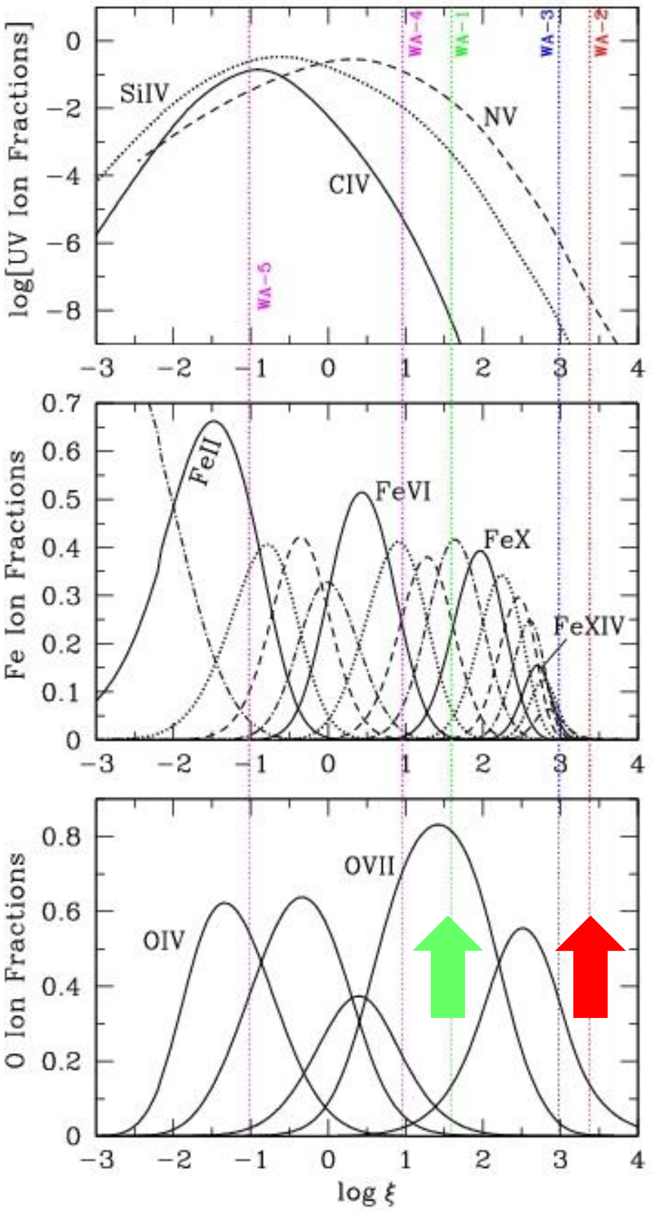

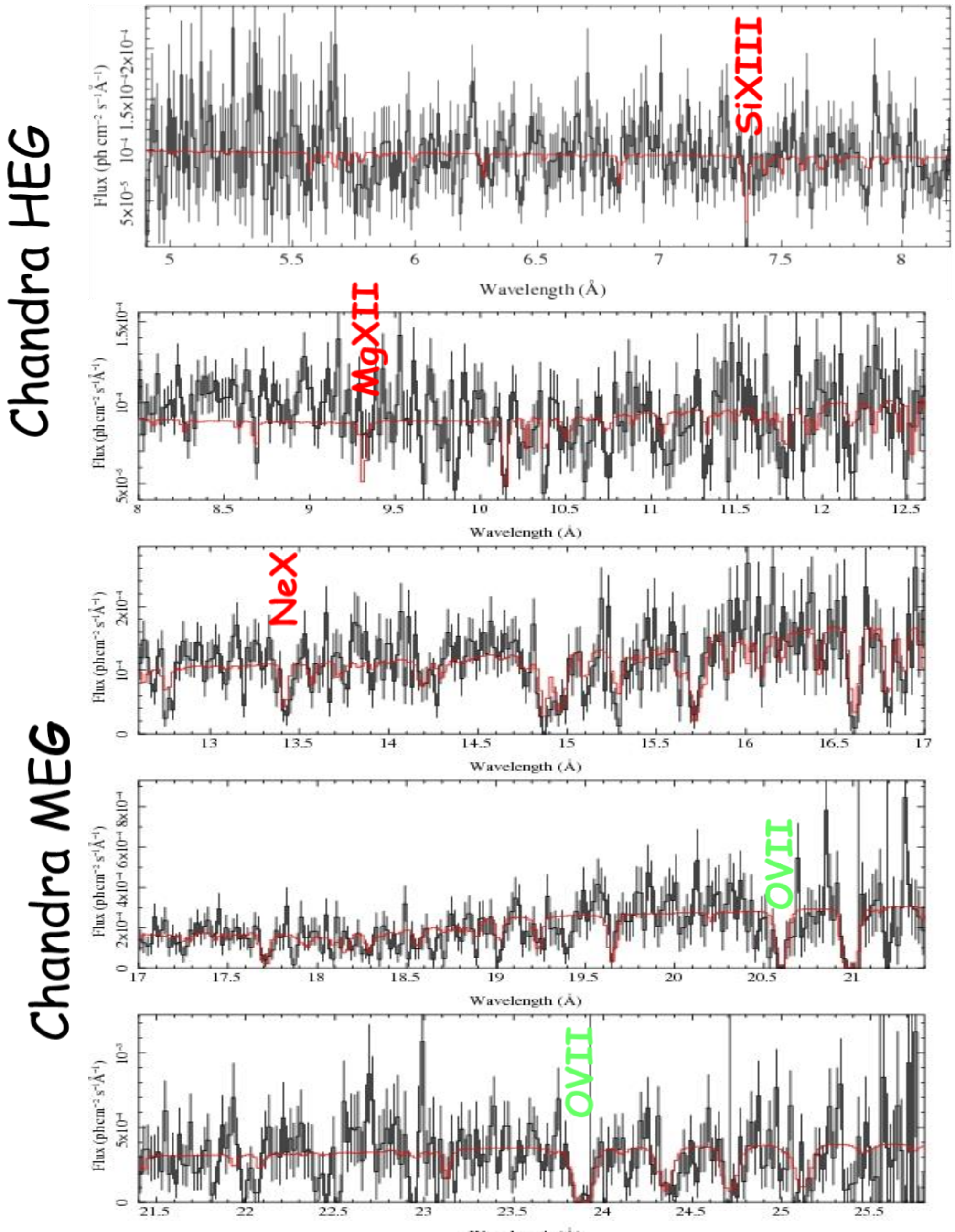

XSTAR warm absorber analysis using `correct' SED

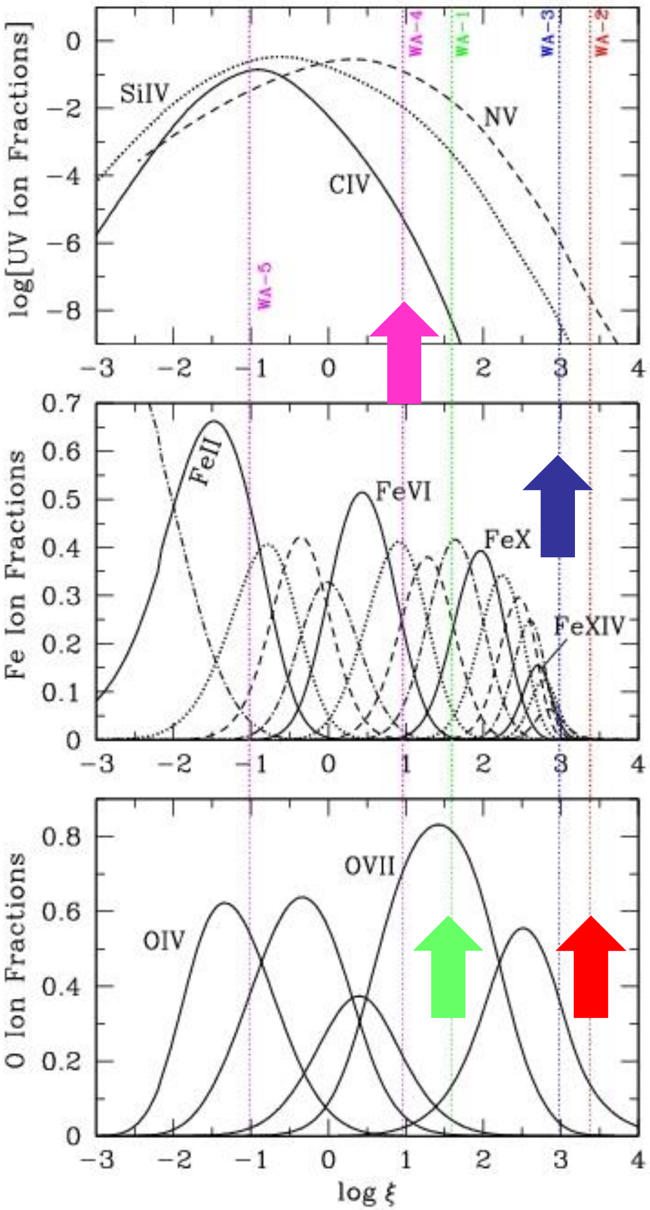

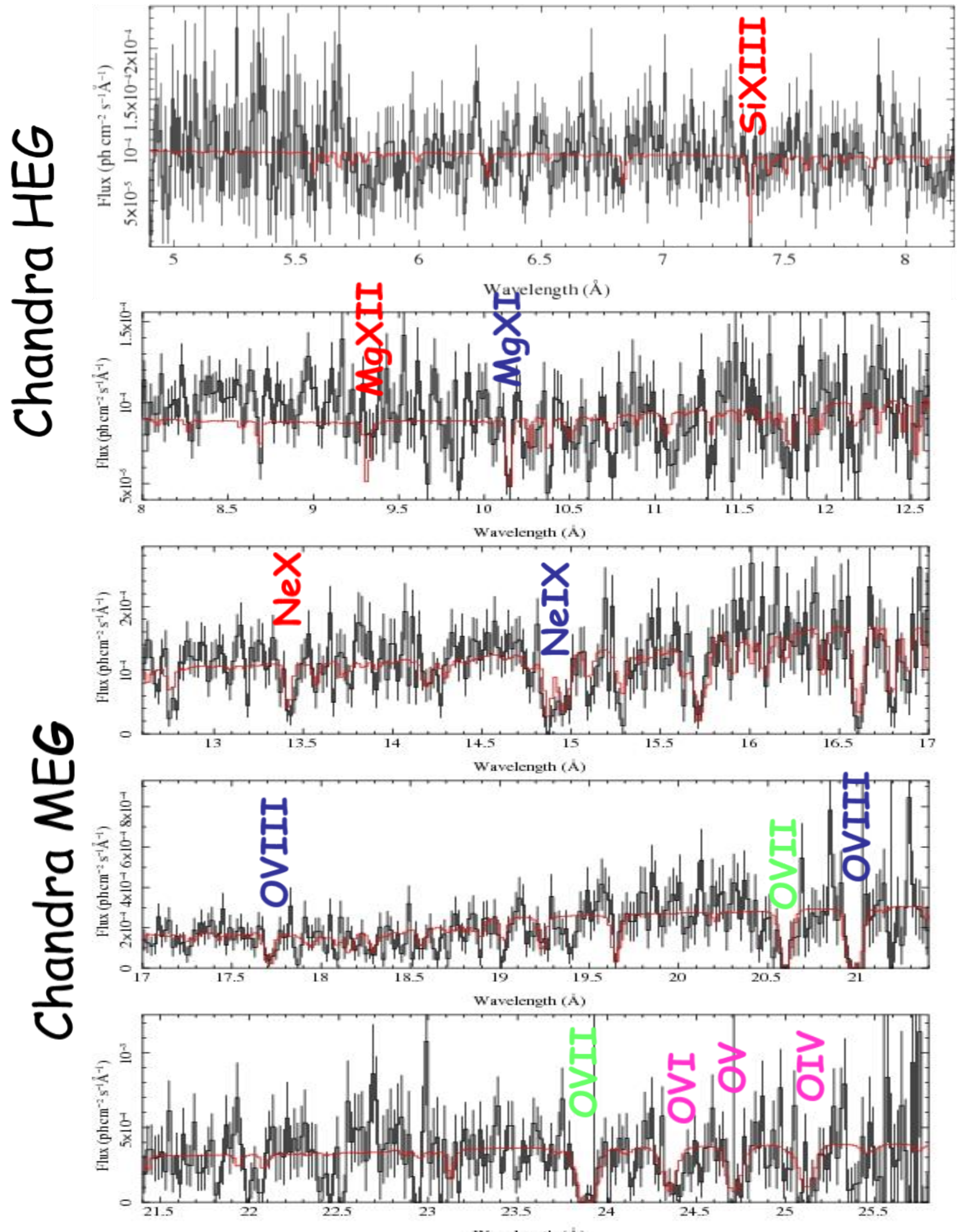

XSTAR warm absorber analysis using `correct' SED

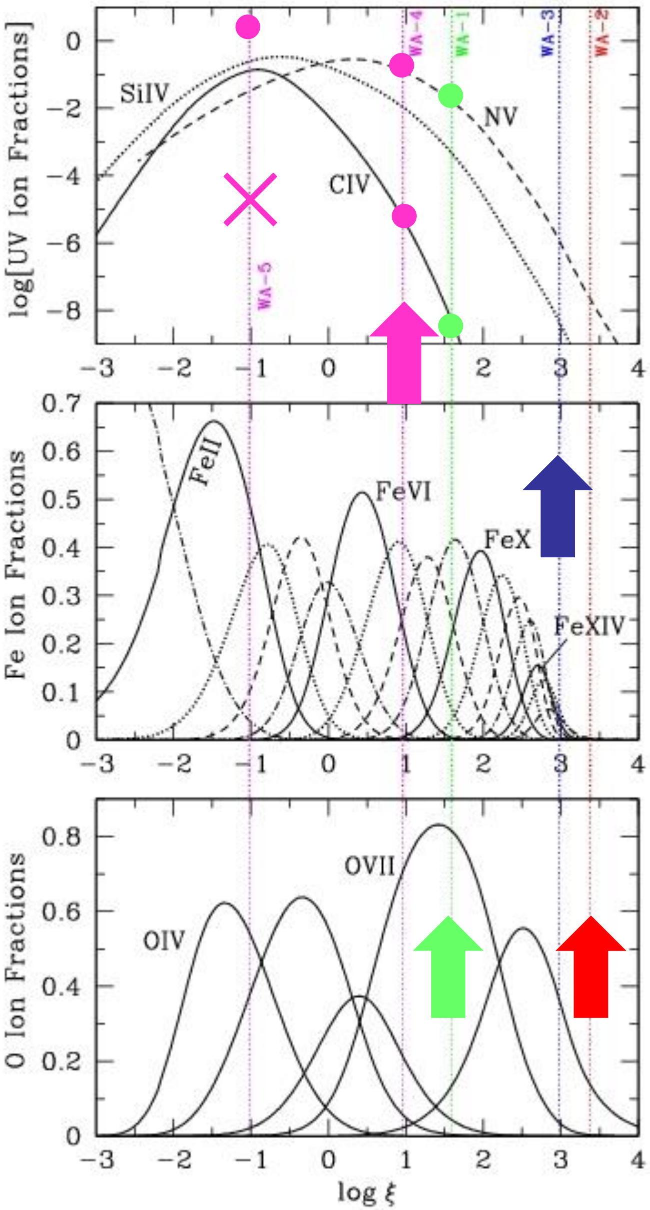

Chandra HEG

Chandra MEG

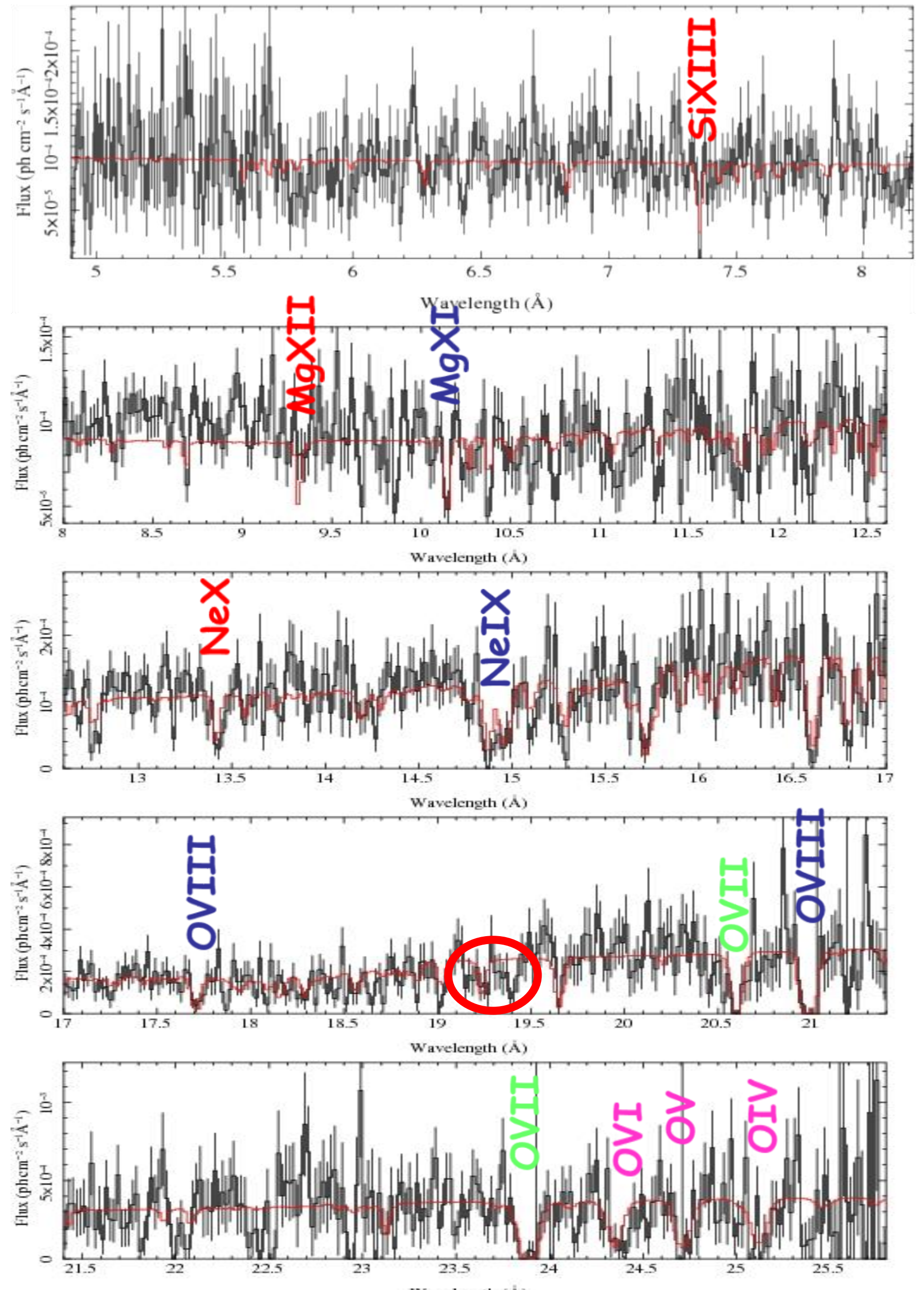

The S-curve for the `correct' SED

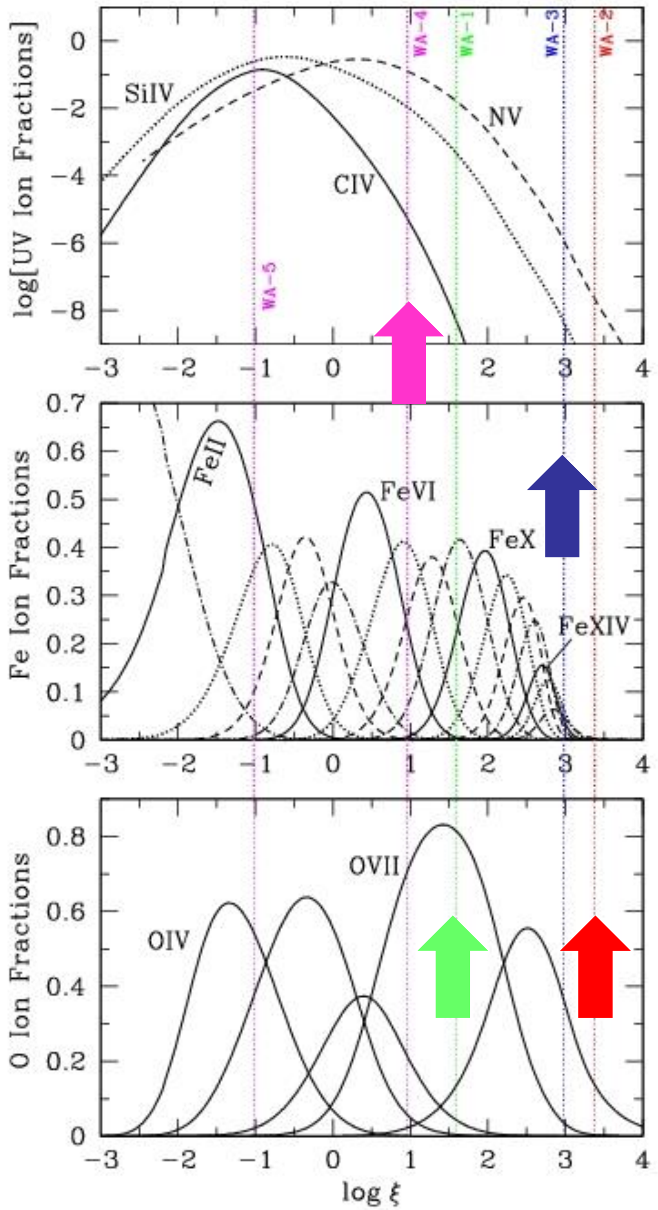

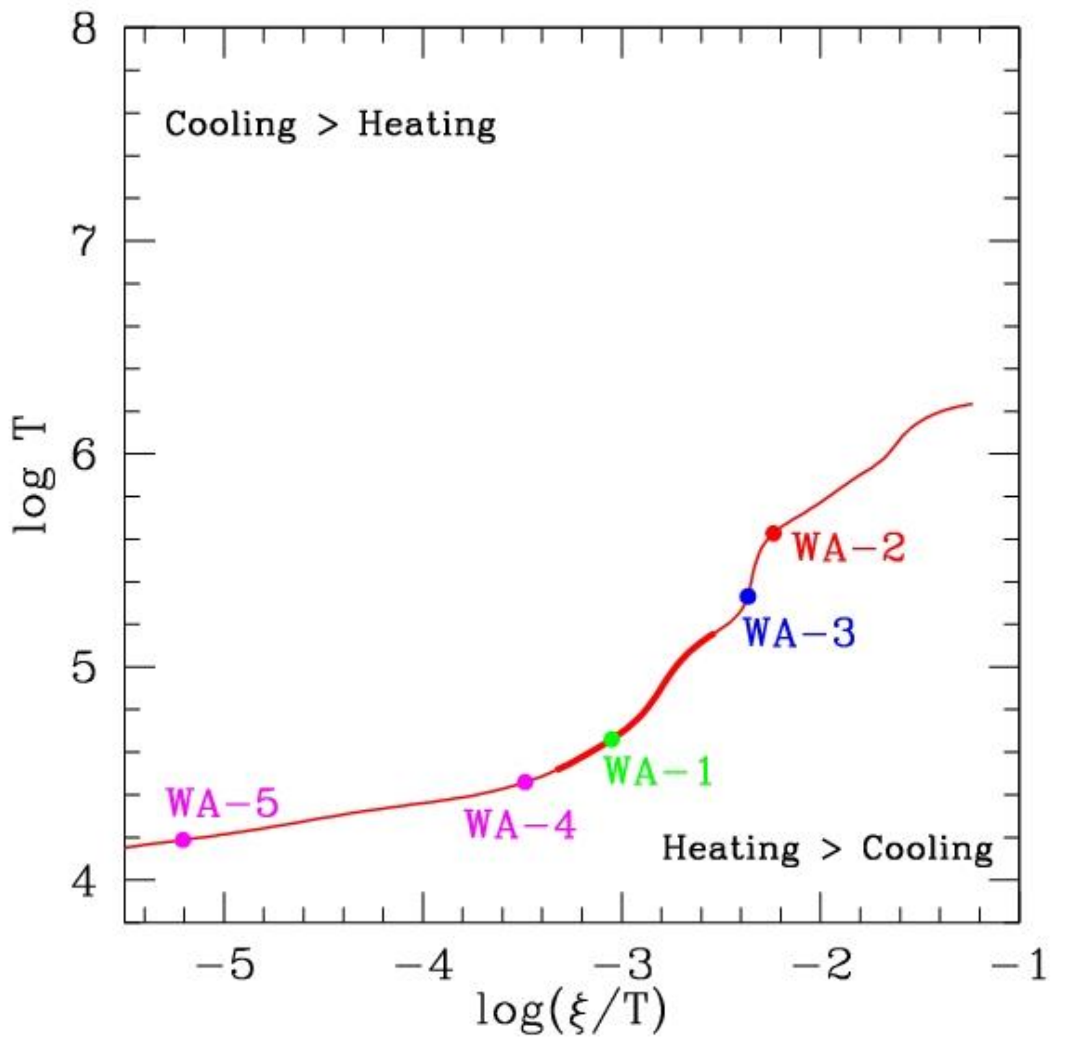

Compare the `correct' and the `incorrect' SED

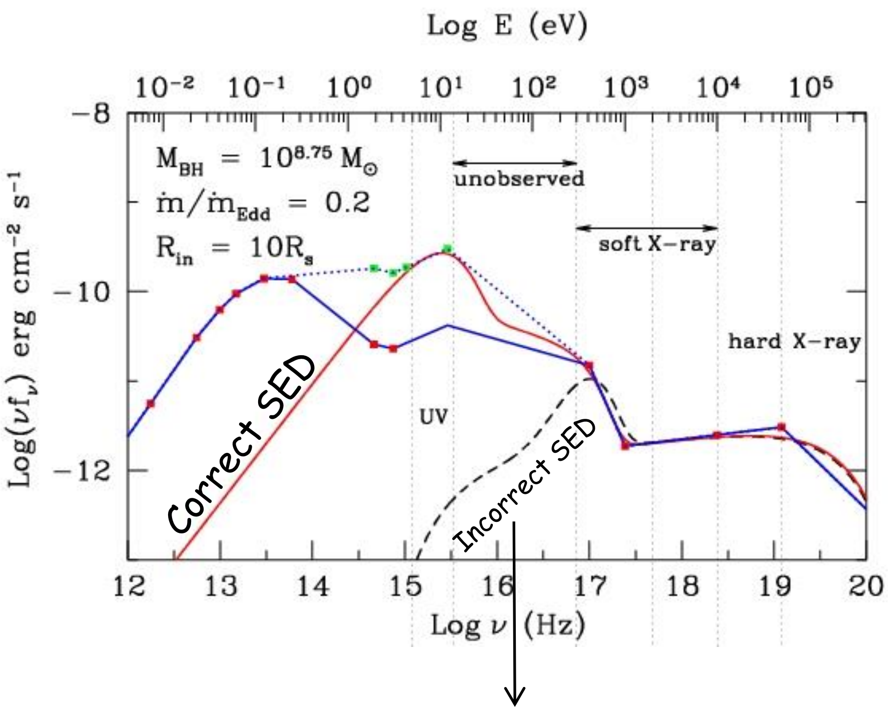

- Holczer et.al. used this SED and argued in favour of discrete WA
- Sako et.al. used similar SED to argue in favour of discrete WA.

See also
Laha et.al. 2013, ApJ, 777, 2
IRAS 13349+2438 in XMM-Newton

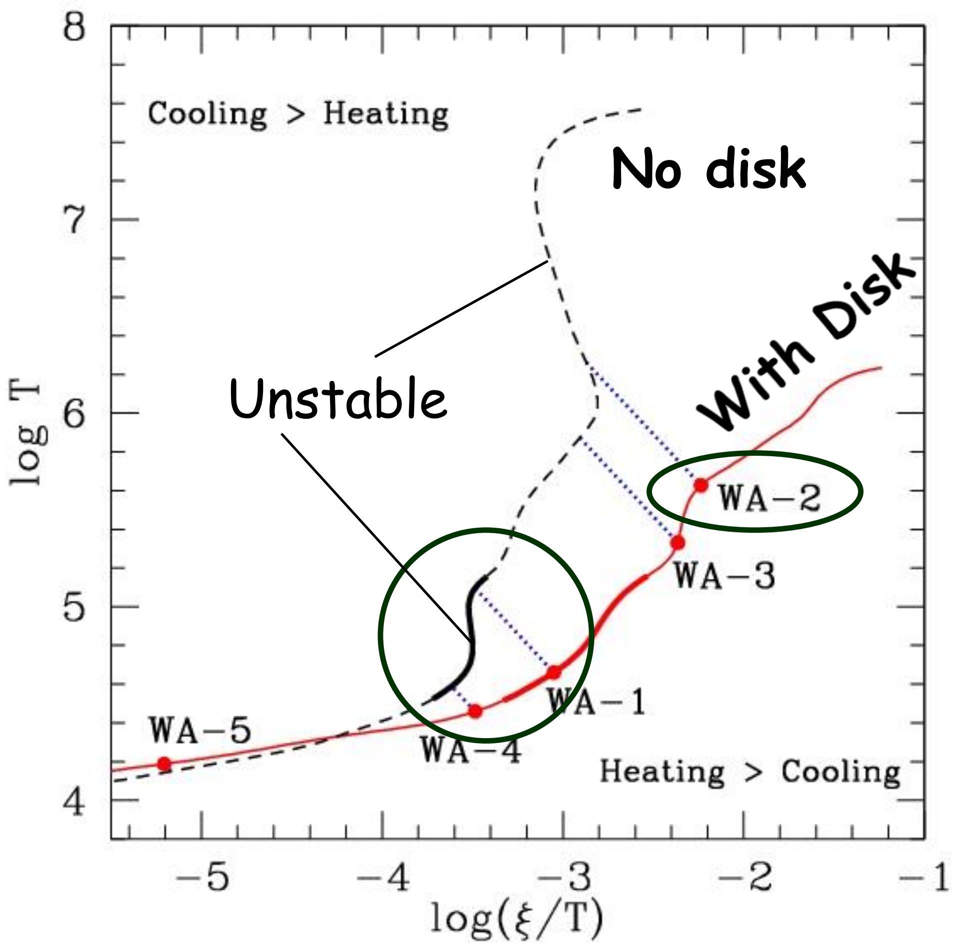

Winds in black hole X-ray binary

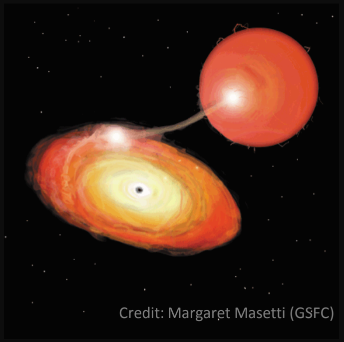

Stellar mass black holes are found in binary systems.

These systems undergo semi-periodic out bursts and become bright in X-rays.

During outburst the observed luminosity performs a “hysteresis” wrt spectral hardness.

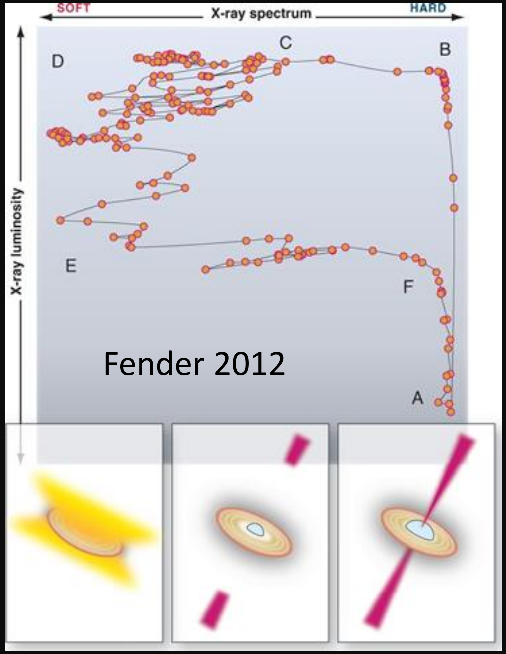

Fender 2012

The binaries pass from Hard to Soft state and back.

The X-ray continuum for the two states are very different.

Winds in black hole X-ray binary

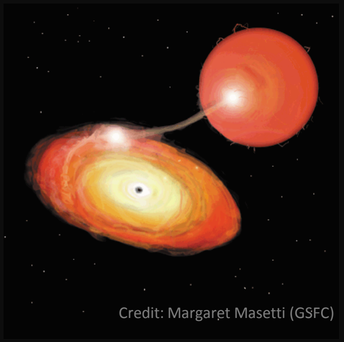

Stellar mass black holes are found in binary systems.

These systems undergo semi-periodic out bursts and become bright in X-rays.

During outburst the observed luminosity performs a “hysteresis” wrt spectral hardness.

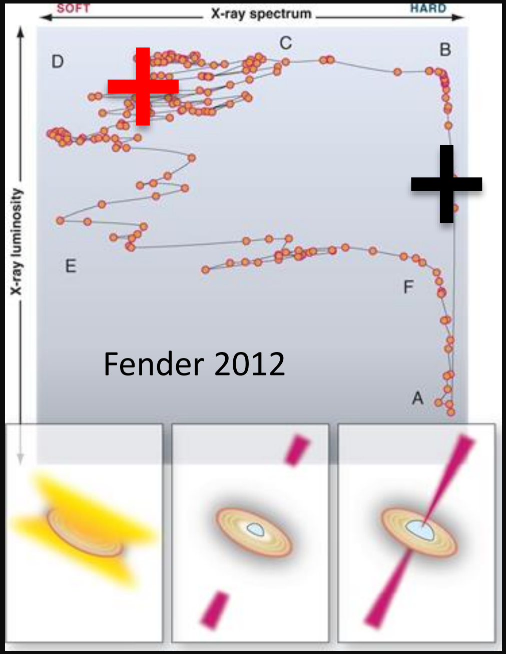

The binaries pass from Hard to Soft state and back.

The X-ray continuum for the two states are very different.

$10M_\odot$ black hole accreting at $0.1\dot{m}_{Edd}$

Thermal –

Diskbb; $r_{in} = 6\ r_g \rightarrow T_{in} = 0.75$ keV
Powerlaw - $\Gamma = 2.5$
$L_{disk}/L_{PL} = 0.8$ in 2 – 20 keV

Hard –

Diskbb; $r_{in} = 20\ r_g \rightarrow T_{in} = 0.39$ keV
Powerlaw - $\Gamma = 1.8$
$L_{disk}/L_{PL} = 0.2$ in 2 – 20 keV

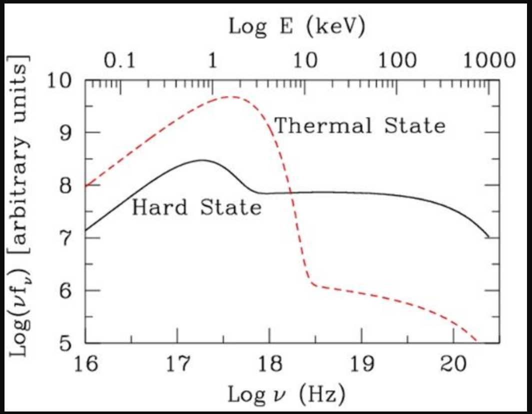

Winds in black hole X-ray binary – an overview

There are 20 confirmed black hole binaries
(Remillar & Mclintock 2006)

But 4 BHBs show absorption lines
(RXTE + Chandra or XMM-Newton)

Most observations show absorption lines from 'only'
FeXXV and FeXXVI (black spectra)

Exceptions (?)

- GROJ1655, 2006 observation (Miller et.al. 2008) – has numerous lines (blue spectra)
- GRS1915, 2000 observation
- (Lee at.al. 2002, Ueda et,al. 2010)

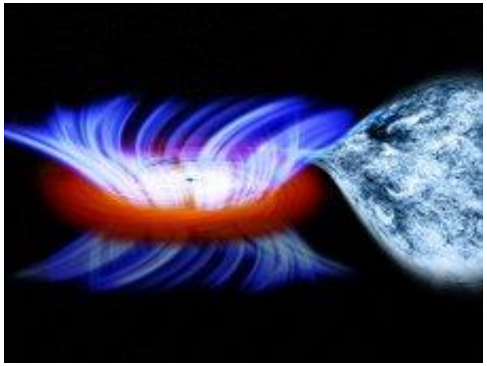

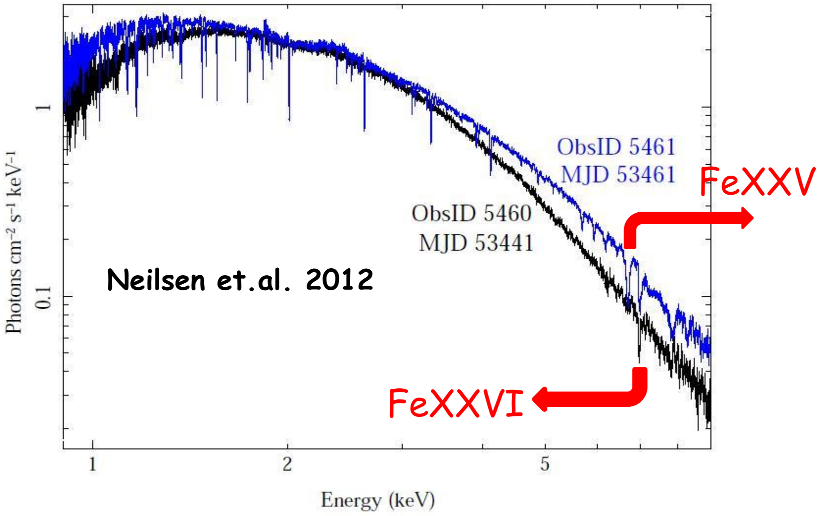

Winds in black hole X-ray binary – an overview

There are 20 confirmed black hole binaries
(Remillar & Mclintock 2006)

But 4 BHBs show absorption lines
(RXTE + Chandra or XMM-Newton)

Most observations show absorption lines from 'only'
FeXXV and FeXXVI (black spectra)

Exceptions (?)

- GROJ1655, 2006 observation (Miller et.al. 2008) – has numerous lines (blue spectra)
- GRS1915, 2000 observation (Lee at.al. 2002, Ueda et,al. 2010)

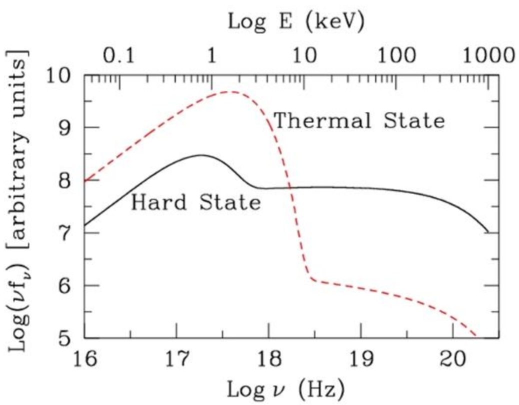

The presence of winds is a "state dependant" effect

Winds are observed in the Soft state

Further, winds are observed in objects of high inclination (i.e. low equatorial angle)

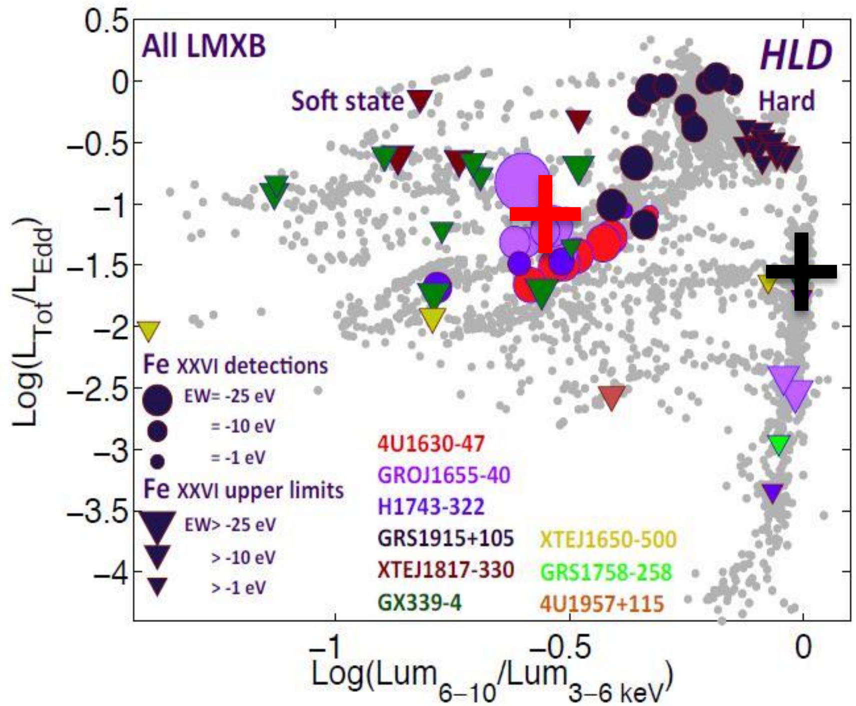

Ponti et.al 2012

MHD winds from the accretion disk: the ANR-Chaos project

(Jonathan) Ferreira, 1997 MHD models are adopted for modeling the wind – providing f(x).
Also Casse & Ferreira 2000 and Ferreira & Casse 2004.

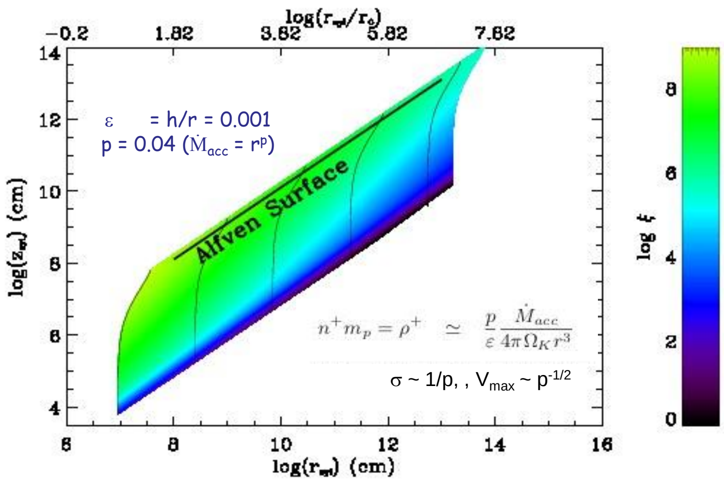

Disk aspect ratio ε (= h/r)
Accretion efficiency p (where $\dot{M}_{acc} = r^p$)

The solutions are self similar. Hence can spread out to large distances.

The ejection or outflow of material is related to the accretion Mechanism - **not** a free parameter (unlike ADIOS scenarios)

$$n(r) = \frac{\dot{m}}{\sigma_T r_g}\left(\frac{r}{r_g}\right)^{(p-3/2)} \quad \text{f(n)}$$

$$v(r) = c\left(\frac{r}{r_g}\right)^{-1/2} \quad \text{f(v)}$$

$$B(r) = \left(\frac{\mu_o m_p c^2}{\sigma_T r_g}\right)^{1/2}\left(\frac{r}{r_g}\right)^{(-5/4+p/2)} \quad \text{f(B)}$$

$$\tau_{dyn}(r) = \frac{2\pi r_g}{c}\left(\frac{r}{r_g}\right)^{3/2} \quad \text{f(dyn)}$$

Can these solutions represent observable winds (in terms of ξ, N_H, n_H and v_{obs}) – both average ones and extreme ones.

Can we recover the (i) state dependent and (ii) angle dependant observability?

If these efforts are successful, then we shall apply the same methods to AGN winds.

Compare the predictions of MHD driven with those from thermally driven models

To find the detectable wind we need CLOUDY calculations

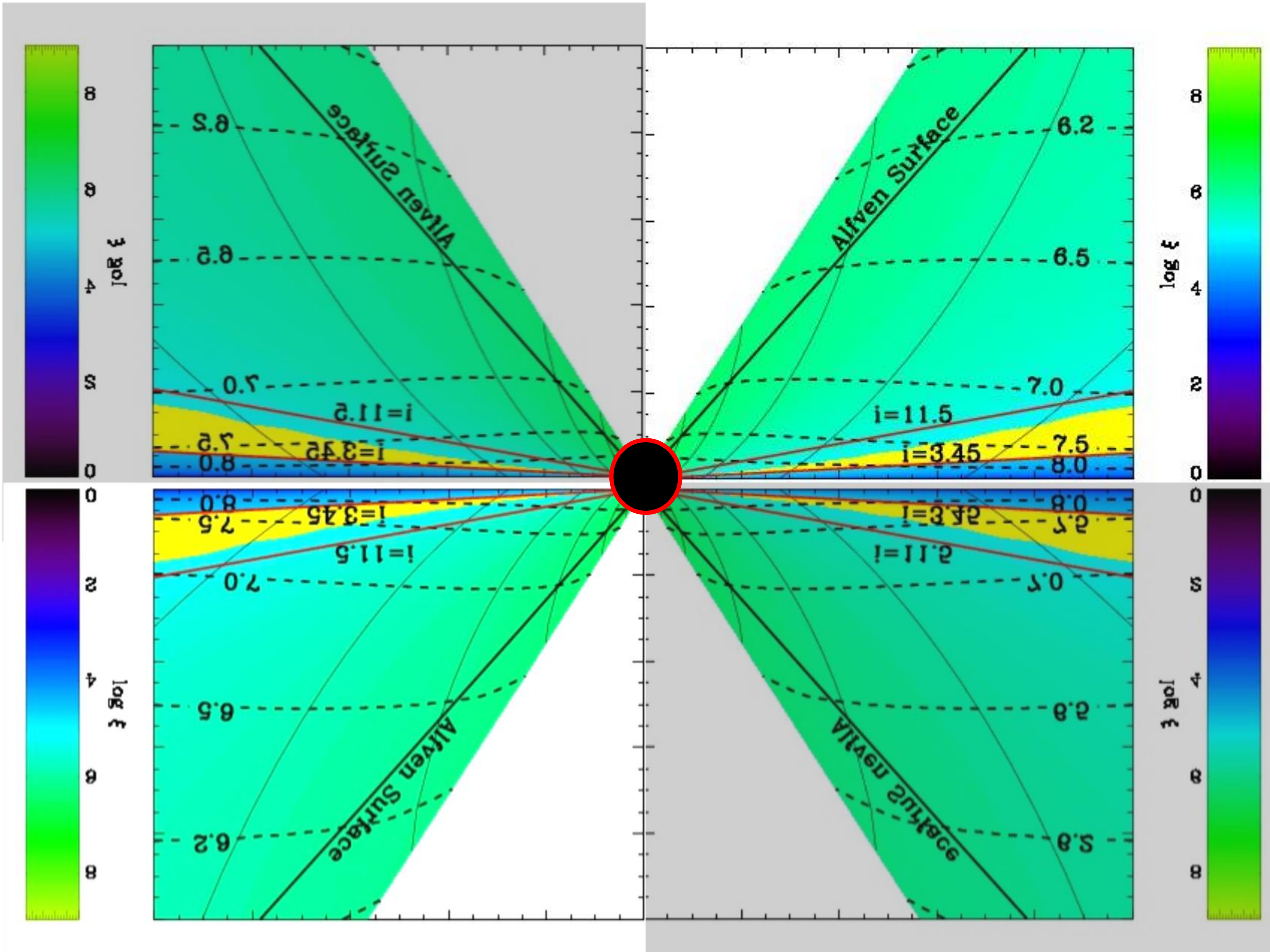

To find the detectable wind we need CLOUDY calculations

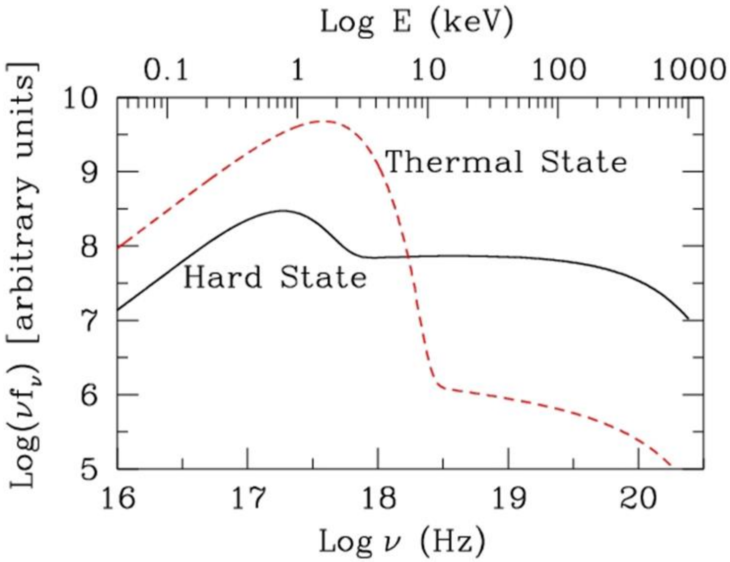

To find the detectable wind we need CLOUDY calculations

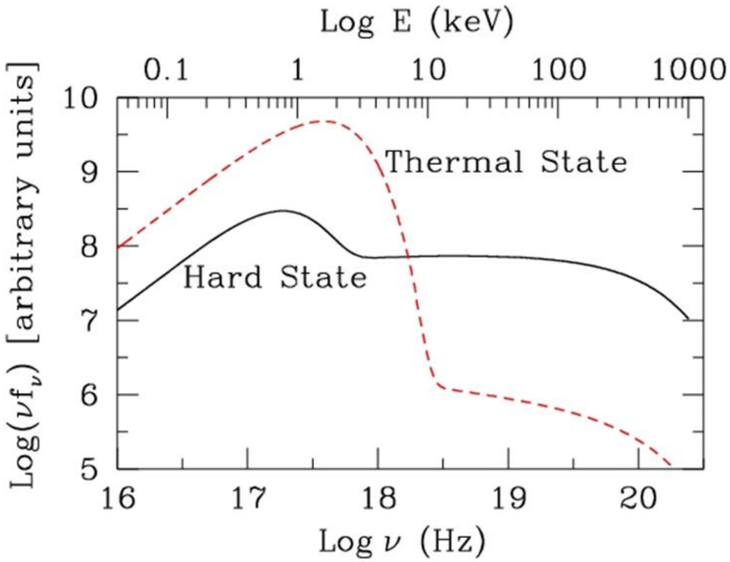

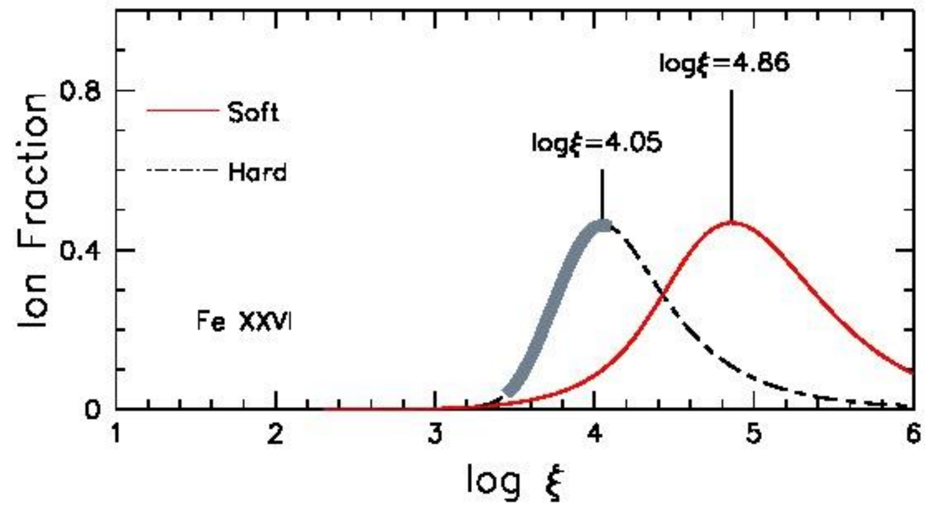

To find the detectable wind we need CLOUDY calculations

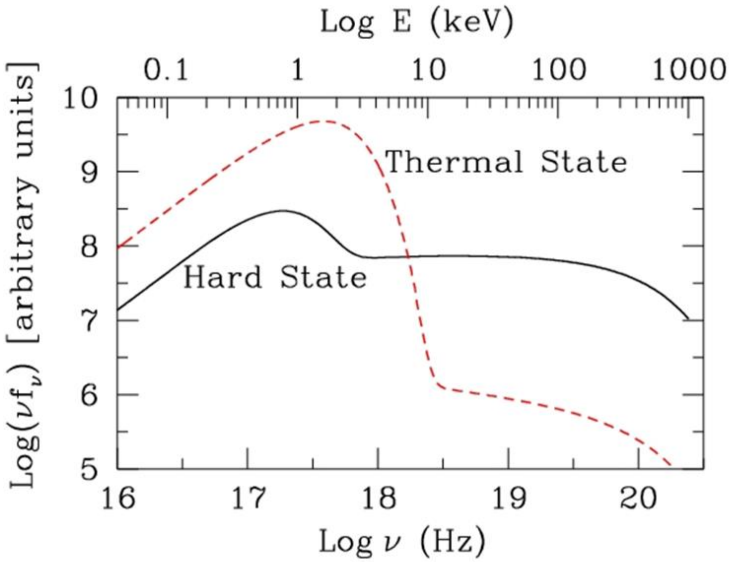

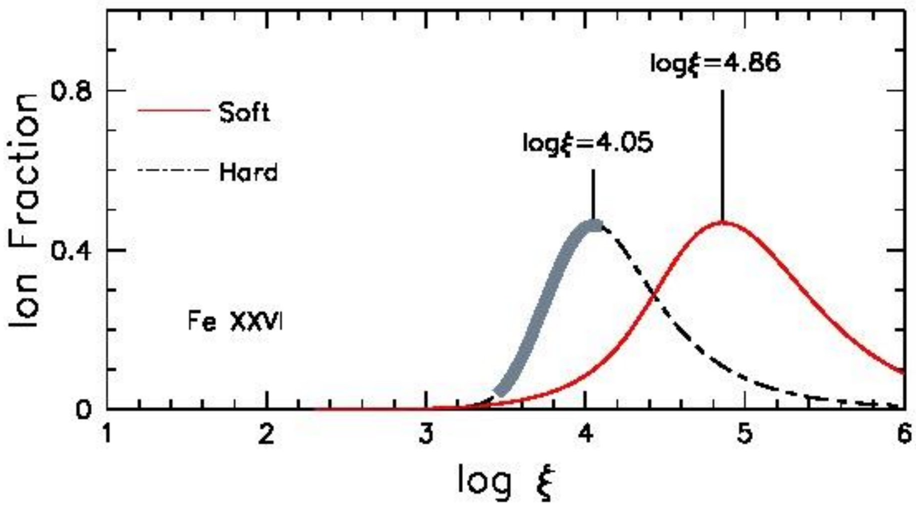

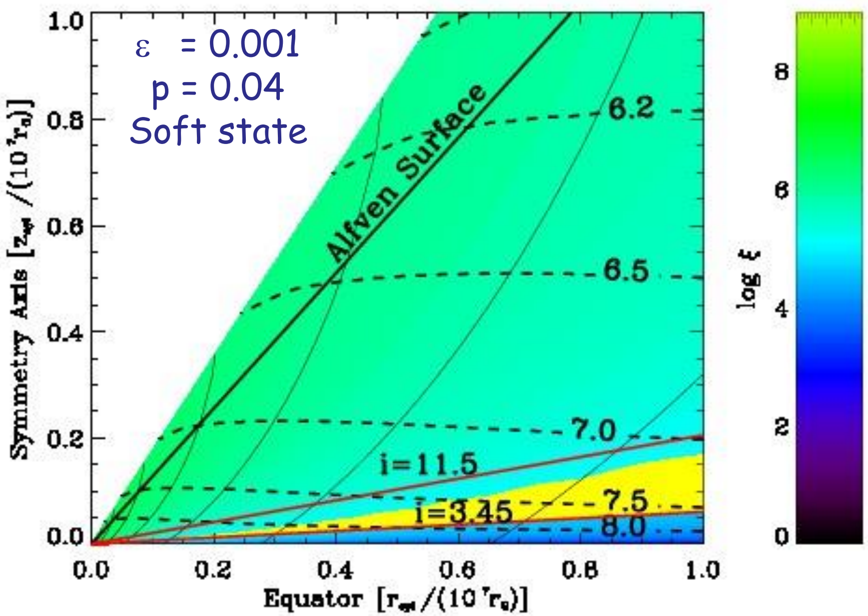

The wind is equatorial

The wind does not exist for Hard State

Strongly agrees with observations

To find the detectable wind we need CLOUDY calculations

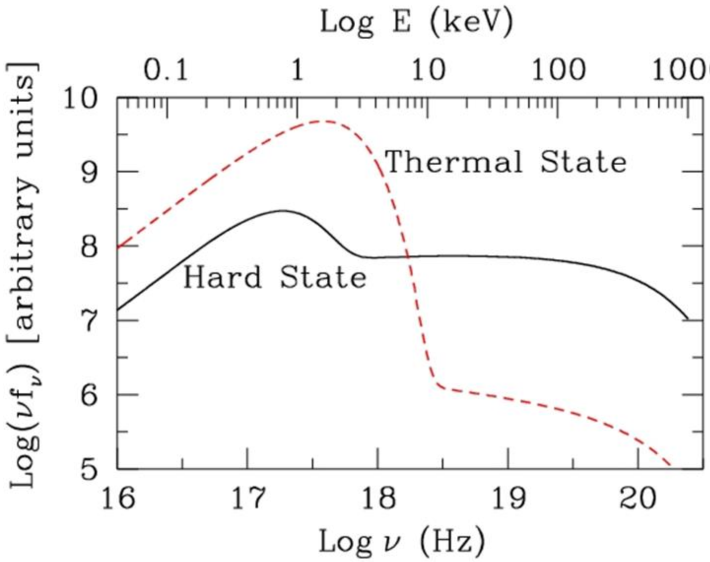

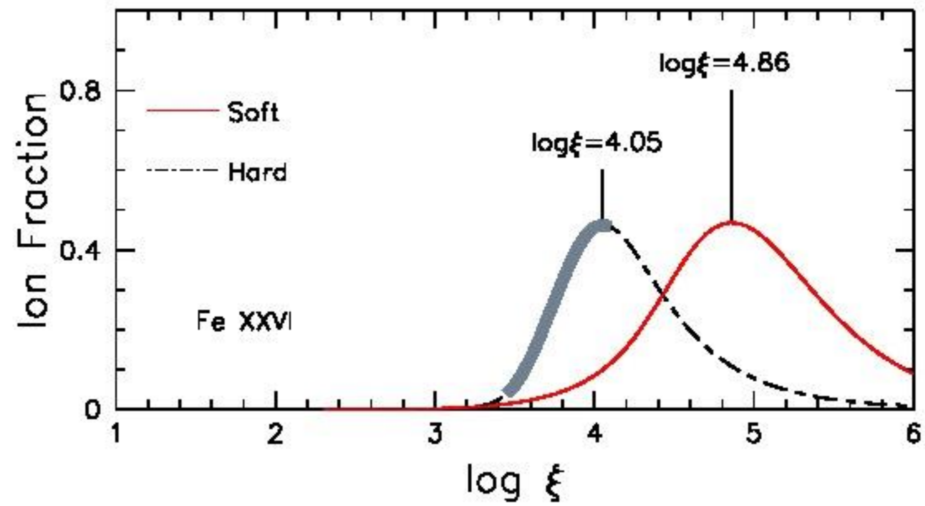

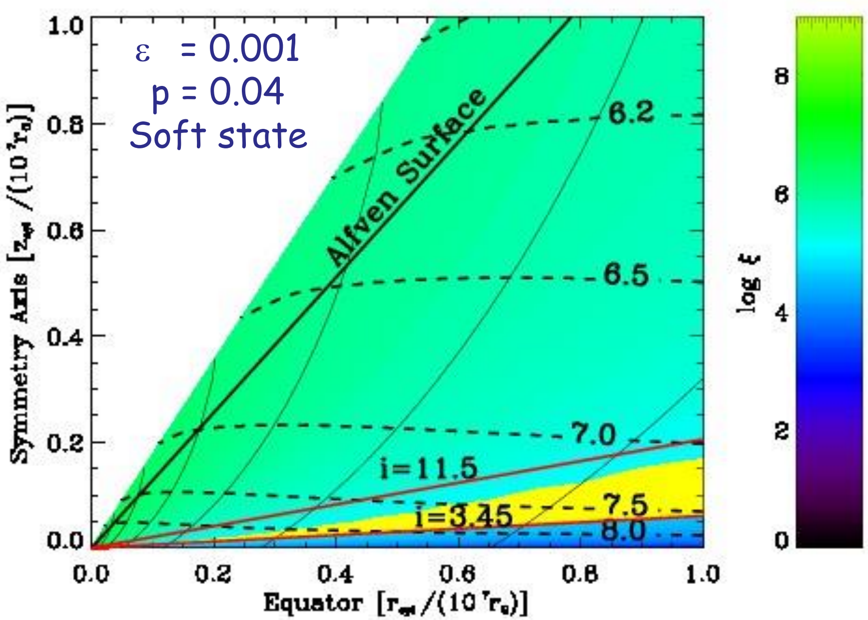

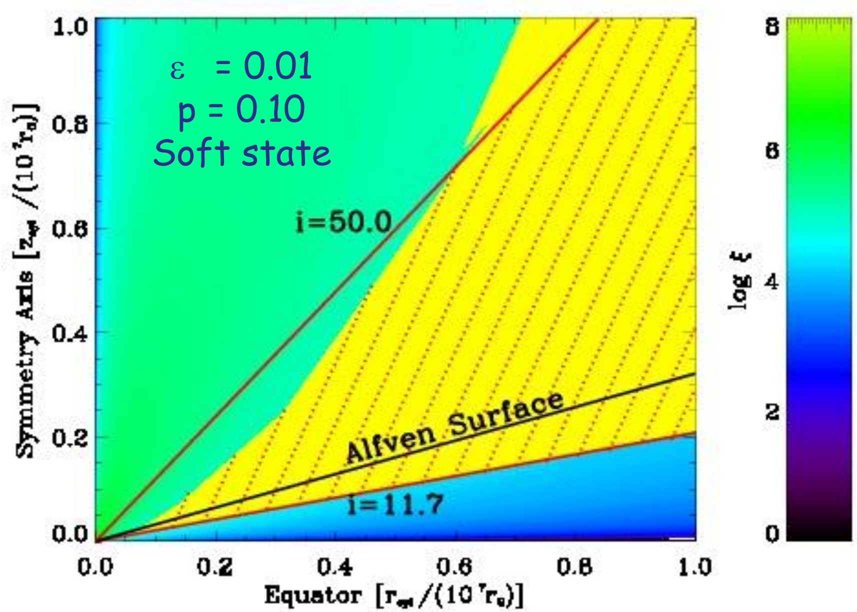

CLOUDY (and similar codes) are powerful

I demonstrated the use of Cloudy and Xstar for handling two very different kinds of analysis in -

- Active Galactic Nuclei (with supermassive black holes) and
- Black hole X-ray Binaries

I hope you enjoyed the show!

But a word of caution given to me by Srianand (when I was young!)

"Do not use CLOUDY like a black box"

CLOUDY has beautiful physics involved – as demonstrated in this workshop
Use it wisely and elegantly.

Thank You

Extras

Warm vs cold magnetic solutions

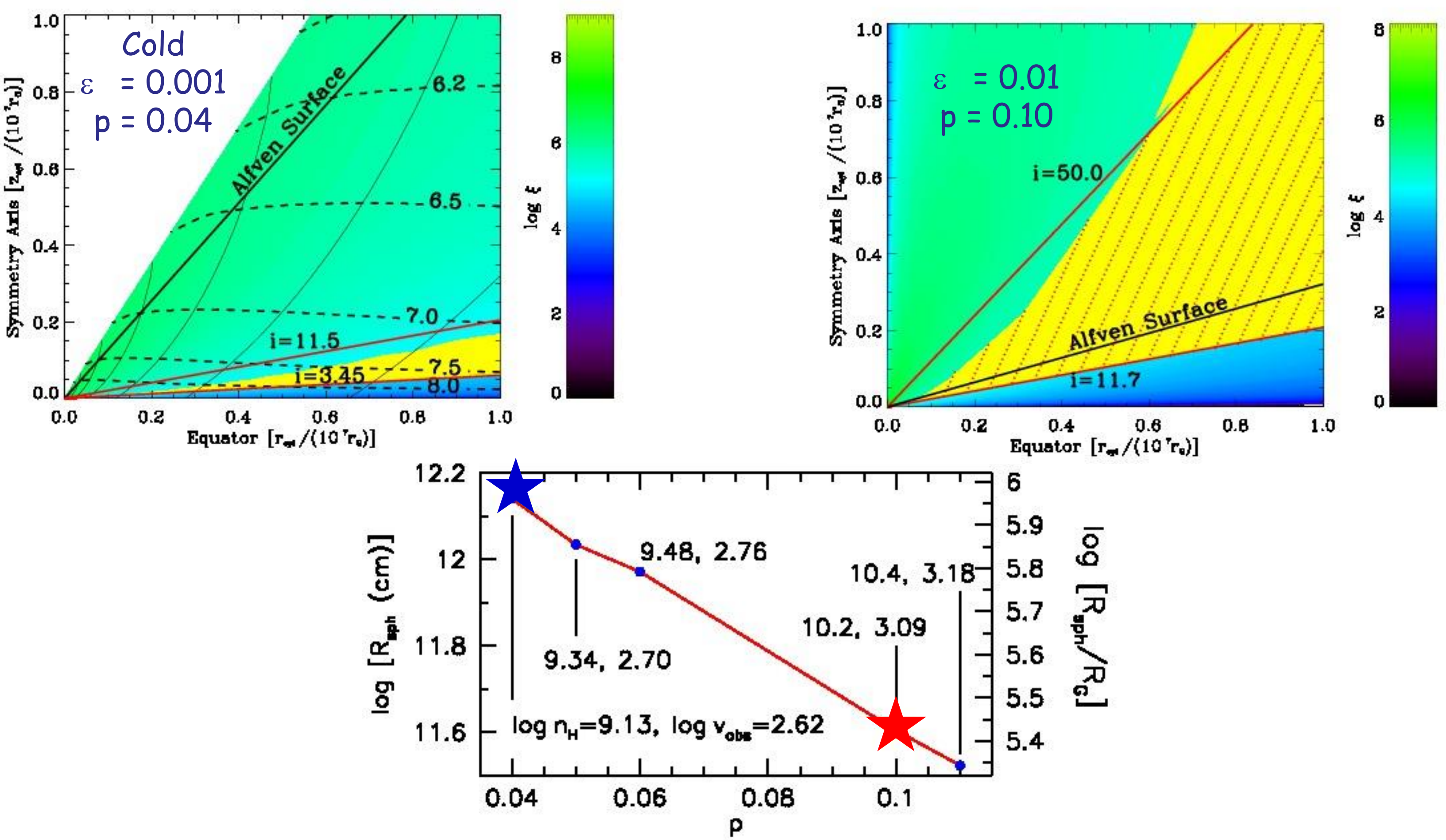

Warm magnetic solutions

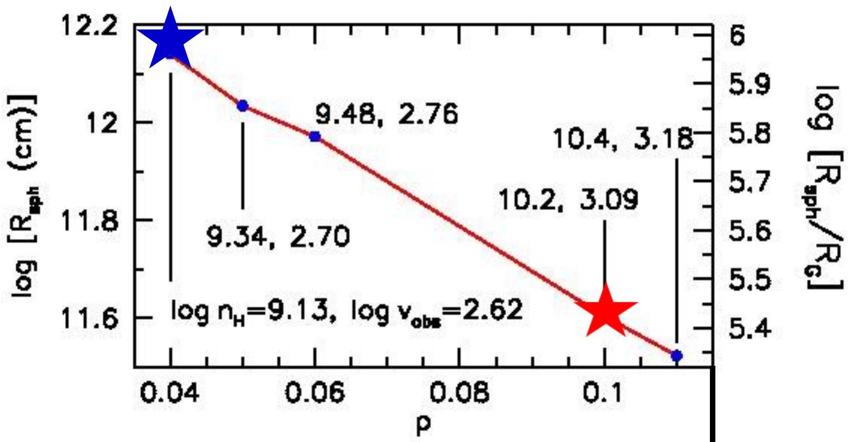

at ~ 5 x 10^4 R_G

at ~ few x 10^3 R_G
log n_H ~ 12.4, log v_{obs} > 4

Warm solution through –
An ad-hoc heating function at disk surface and base of wind
p increased by increasing normalisation
For $\varepsilon = 0.01$, $p \leq 0.11$.

Why do we need higher p?
Wind still at $R_{sph} > 10^5\ R_g$ and $n_H \sim 10^{10}$ cm^{-3}
GROJ1655 needs $R_{sph} \sim 10^3\ R_g$ because $n_H > 10^{12}$ cm^{-3}

Fukumura et.al. papers - p ~ 0.5, to explain AGN winds
Casse & Ferreira 2004 - p ~ 0.45 to explain YSO winds

A rough linear extrapolation puts the wind at 5x10^4 R_G (if p = 0.5)

Choice of ξ upperlimit decides the results we get.
We had chosen a rather stringent upperlimit, log ξ < 5.11
Relaxing it to log ξ < 6 brings the wind closer by ~ 30 times
(actual calculations on ε = 0.01 and p = 0.10 solution)